The Evolution of Synthetic Aperture Radar Systems and their Progression to the EOS SAR

JoBea Way, *Member, IEEE,* and Elizabeth Atwood Smith

***Abstract*—The spaceborne imaging radar program of the National Aeronautics and Space Administration (NASA) has evolved primarily through Seasat and the Shuttle Imaging Radar (SIR) to a multifrequency, multipolarization system capable of monitoring the Earth with a variety of imaging geometries, resolutions, and swaths. In particular, the ability to digitally process and calibrate the data has been a key factor in developing the algorithms which will operationally provide geophysical and biophysical information about the surface of the Earth using synthetic aperture radar (SAR). This paper describes the evolution of the spaceborne imaging radar starting with the Seasat SAR, through the SIR-A, SIR-B, and SIR-C/X-SAR missions, to the EOS SAR which is scheduled for launch as part of the Earth Observing System (EOS) at the end of the 1990s. A summary of the planned international missions, which may produce a permanent active microwave capability in space starting as early as 1991, is also presented, along with a description of the airborne systems which will be essential to the algorithm development and long-term calibration of the spaceborne data. Finally, a brief summary of the planetary missions utilizing SAR and a comparison of their imaging capabilities with those available on Earth is presented.**

I. Introduction

In 1978, the first Earth-viewing spaceborne synthetic aperture radar (SAR) was launched into orbit on the Seasat spacecraft. The success of Seasat led to a series of Shuttle Imaging Radar (SIR) missions designed to progressively develop a SAR with the features necessary to provide key measurements of biophysical and geophysical properties (Table I; [1]) of the Earth. Through these shuttle missions and airborne SAR and ground-based scatterometer experiments, a permanently orbiting SAR has been defined as a three-frequency (L-, C-, and X-band), multipolarization radar with variable resolution (30–250 m), variable swath width (30–500 km), and selectable incidence angles ranging from 15 to 50°. This SAR will fly as part of the Earth Observing System (EOS) series in the late 1990s and will provide a 15-year data set in the active microwave region (EOS SAR Instrument Panel Report, 1988).

In the interim, the European Space Agency (ESA), Japan, Canada, and the Soviet Union are building single-channel SARs which are being placed in orbit for 2–5-year periods starting in 1991. These include the ESA Remote Sensing (ERS-1) satellite, the Japanese Earth Resources Satellite (JERS-1), the Canadian RADARSAT, and the Soviet Union's Almaz-1. Parallel efforts to launch SARs to cloud-shrouded planets and moons are also underway. These include the Magellan mission to Venus, which was launched in 1989, and the CRAF/Cassini mission to Titan scheduled for launch in the mid 1990s. This paper describes the radars, the data systems and the mission designs for these SAR systems.

TABLE I
Biophysical and Geophysical Products for the EOS SAR

Observation Parameter	Units
Vegetation type	Class
Vegetation extent (deforestation)	Extent (m^2), % change
Vegetation biomass	Mass/area (kg/km^2)
Canopy geometry	Angular and linear (deg, m)
Vegetation water content	% by volume
Vegetation water potential	Bars
Soil moisture (vegetated)	% by volume
Soil moisture (bare soil)	% by volume
Land-water boundaries/floods	Area (m^2)
Drainage patterns	Linear extent (m)
Snow water equivalent	Height (cm)
Snow extent (wet or dry)	Areal extent (m^2)
Sea ice extent	Location (lat/long)
Sea ice concentration	Fraction
Sea ice type	Class
Sea ice motion	Velocity (km/day)
Ice sheet, lake and river ice extent	Location (lat/long)
Ice sheets and shelf dynamics	Velocity (m/year)
Current, fronts, eddies	Location (lat/long)
Internal waves	Location (lat/long)
Surface wind field	Velocity (m/s)
Surface waves	Length (m), direction (deg)
Surface wave height	Height (m)
Surface roughness (nonvegetated)	RMS height (cm)
Surficial material boundaries	Extent (m)
Topography	Height (m)
Erosion	Area (m^2)
Landform patterns	Area (m^2)
Sand depth	Depth (m)

II. Spaceborne Imaging Radars

In order to reach the EOS era with an advanced SAR, the shuttle is being used as a test bed for developing increasingly more complex radars. The three major components of a radar system, the antenna and electronics, the data system, and the mission design, have advanced

Manuscript received August 13, 1990; revised April 21, 1991. This work was performed under contract with the National Aeronautics and Space Administration.

The authors are with the Jet Propulsion Laboratory, California Institute of Technology, Pasadena, CA 91109.

IEEE Log Number 9102504.

TABLE II
THE US SPACEBORNE MISSIONS

	Seasat SAR	SIR-A	SIR-B	SIR-C/X-SAR	EOS SAR
Imaging Characteristics					
Band (wavelength, cm; frequency, GHz)	L(23.5, 1.275)	L(23.5, 1.278)	L(23.4, 1.282)	L(23.9, 1.25) C(5.7, 5.3) X(3.1, 9.6)	L(23.9, 1.25) C(5.7, 5.3) X(3.1, 9.6)
Polarization	HH	HH	HH	quad (L, C) VV (X)	quad (L), HH, VV (C, X)
Look (Incidence) Angle	20° (23°)	47° (50°)	15°-60° (15°-64°)	(15°-55°)	(15°-45°)
Azimuth Resolution (m)	25	40	25	25	20-250
Range Resolution (m)	25	40	58-17	60-10	8-250
Looks	4	6	4	4	4
Swath width (km)	100	50	10-60	15-60	30-360
Special Modes			squint, spotlight	squint, spotlight, scanSAR	scanSAR
Instrument Characteristics					
Antenna Type	corporate feed	corporate feed	corporate feed	phased array	phased array
Antenna Size (m × m)	2.16 × 10.7	2.16 × 9.4	2.16 × 10.7	(2.95 + 0.75 + 0.40)*** ×12	(1.9 + .49 + .26)*** ×10.8
DC Power (kW)	1.2	1.0	1.2	3.9 (L-band) 2.4 (C-band)	5.8 (peak) 1.5 (avg)
Bandwidth(s) (MHz)	19	6	12	40, 20, 10	20, 10, 5
Noise equivalent sigma-0***	−24	−32	−28	−48/−36/−28	−36/−27/−22
Orbit Characteristics					
Altitude (km)	800	259	224*†	~225	620
Inclination	108°	38°	57°	57°	98°
Sun Synchronous	no	no	no	no	yes
Equator Crossing Time	—	—	—	—	1:30-4:00 p.m.
Daytime Node	variable	descending	descending	descending	ascending
Exact Repeat (days)	17 (June 27-Aug 25) 3 (Aug 25-Oct 10)	—	—	—	16
Approx. Repeat (days)	3 (June 27-Aug 25)	1	1	1	5
Mission Characteristics					
Spacecraft	Seasat	Shuttle (Columbia, STS-2)	Shuttle (Challenger, 41-G)	Shuttle	Dedicated Satellite
Launch Date	June 27, 1978†**	November 12, 1981	October 5, 1984	1993, 1994, 1996	1999
Mission End	October 10, 1978	November 14, 1981	October 13, 1984	—	2014
Mission Duration	100 days	2.4 days	8.3 days	8.3 days each	15 years
Data Characteristics					
Data Rate (Mbps)	110	—	30†	240/recorder 45 through TDRS	180 (peak) 15 (average)
Recording Options	digital	optical	optical, digital/TDRS	digital/TDRS	digital/TDRS
Onboard Recorder Capacity	—	8 h	20 min/tape, 7 tapes	30 min/cassette ~100 cassettes	TBD
Operation Time	42 h	8 h	7 h (digital) 8 h (optical)	60 h	25% duty cycle
Coverage (million sq. mi.)	100	10	15	TBD	global/5 days
Processing					
Type	optical/digital	optical	optical/digital	digital	digital
Location	JPL	JPL	JPL	JPL, DLR	EOS DAACs
Other Sensors	Microwave Radiometer, Scatterometer, Radar Altimeter, V/IR Radiometer	MAPS, FILE, SMIRR, others	ERBE satellite, MAPS, FILE	MAPS	EOS

***L-, C- and X-bands at 50° for SIR-C/X-SAR and 40° for EOS SAR.
*†initially at 354 km for first 22 orbits, 257 km for next 11 orbits and finally 224 km for remainder of mission
†45 Mbps direct downlink through TDRS also possible but TDRS link failed
†**at 01:12:44 GMT, Day 178

depending on technology, launch vehicle capabilities, and available funding. The evolution of each of these components is described in the following sections and summarized in Table II.

A. SEASAT SAR

The spaceborne imaging radar program began in 1978 when the first SAR was launched into orbit aboard the Seasat spacecraft [2]-[4]. The Seasat SAR was specifically dsigned to optimize imaging of the ocean (Fig. 1(a)).

1. Instrument. The selected frequency and polarization for the Seasat SAR were L-band (1.275 GHz) and HH (horizontally transmitted, horizontally received), respectively, and a look angle of 20° was chosen because of the sharp fall-off in backscatter at higher incidence angles over the ocean. From the Seasat altitude of 800 km, a 1-kW peak power was required to obtain a good signal to noise ratio (SNR) at the 23° incidence angle. The antenna was a corporate feed system and was 2.16 by 10.7 m in size divided into nine panels. It was folded for launch in an accordion fashion and deployed permanently once

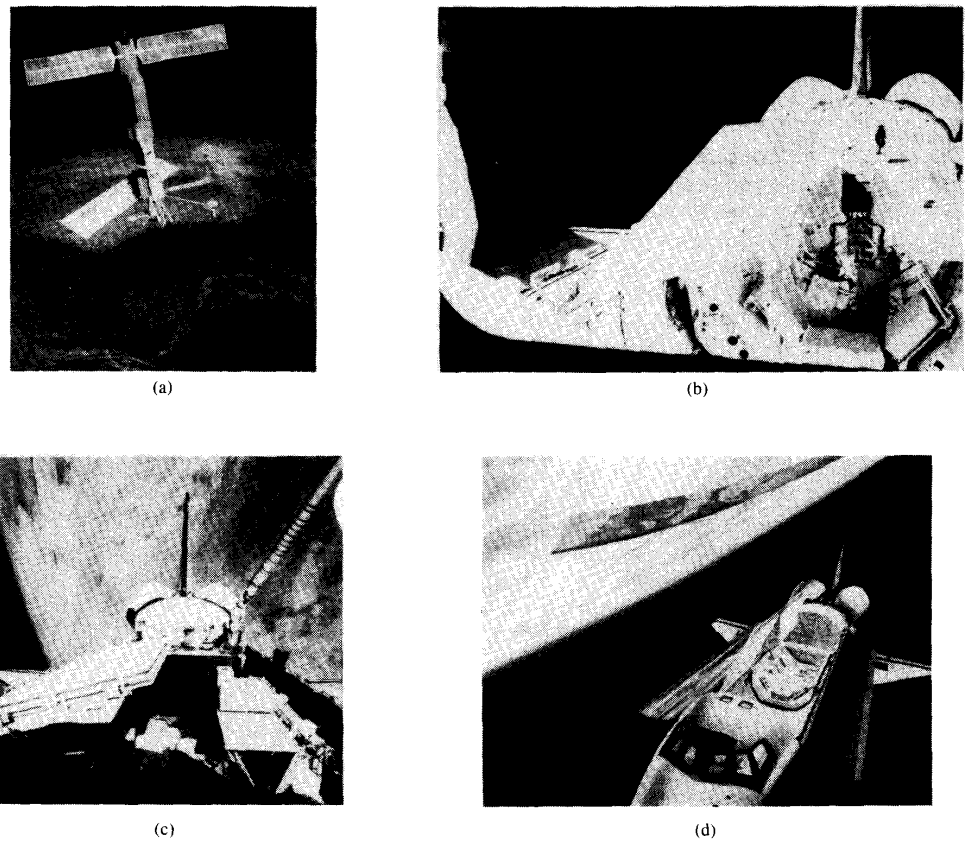

(a) (b) (c) (d)

Fig. 1. The U.S. spaceborne imaging radar instruments on Seasat and the shuttle including (a) the Seasat SAR, (b) SIR-A, (c) SIR-B, and (d) SIR-C/X-SAR.

orbit was achieved. The resolution of the Seasat SAR imagery is 25 by 25 m (4 looks) and the swath width is 100 km, still the widest swath ever acquired from orbit. Imagery obtained from the Seasat SAR clearly demonstrated its sensitivity to surface roughness, slope, and land–water boundaries. Seasat SAR images have been used to determine the directional spectra of ocean waves, surface manifestations of internal waves and mesoscale eddies, polar ice motion, geological structural features, soil moisture boundaries, vegetation characteristics, and land-use patterns. Key results are summarized by [5]–[15].

2. Data system. One of the greatest challenges in designing a SAR is the data system. Because SARs are high resolution, wide swath, multimode imagers, data rates are extremely high. In addition, in order to reduce speckle, SAR data rates are higher than visible and infrared imagers with the same swath, resolution, and number of bands by a factor of the number of looks (usually four). Finally, complex phase data are transmitted to the ground to be processed into images. All these factors contribute to making the SAR data rates high.

The Seasat SAR transmitted its data in an analog format to ground receiving stations distributed over North America and Europe [3], [16]. (Fig. 2). The data were recorded digitally and the complete Seasat SAR data set was processed optically. Selected scenes were then processed digitally in a 100 by 100 km format [17]. Approximately 1500 scenes have been processed digitally to date and some of these data have been digitally mosaicked to provide high resolution synoptic views of Alaska (38 scenes, 440 by 660 km region) and southern California (33 scenes, 400 by 600 km region) [18].

3. Mission design. The Seasat mission was designed to optimize coverage of the ocean and ice; therefore, an orbit altitude of 800 km and an inclination of 108° were selected (Fig. 3). Seasat was launched from Vandenburg Air Force Base in California on June 27[1], 1978, and acquired data for a period of 3-1/3 months. The orbit during the first 2 months was a 17-day exact repeat with a

[1](June 28 in (GMT).

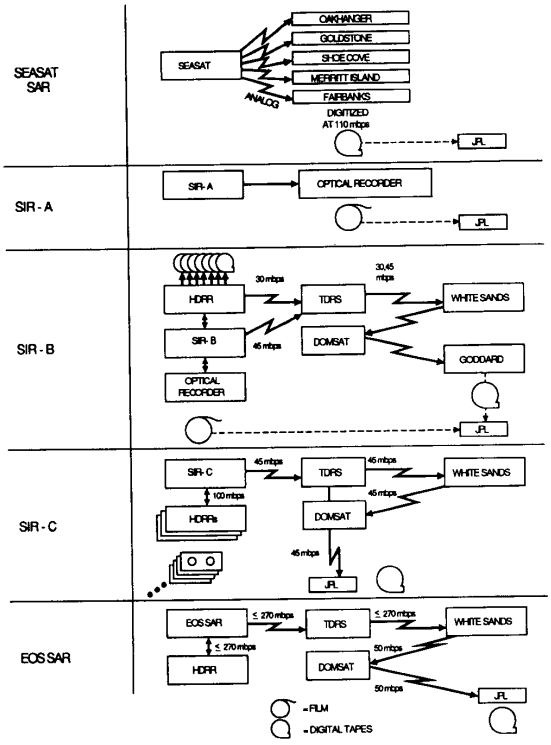

Fig. 2. The evolution of the data systems for the U.S. spaceborne missions from the Seasat SAR through the EOS SAR including SIR-A, SIR-B, and SIR-C/X-SAR.

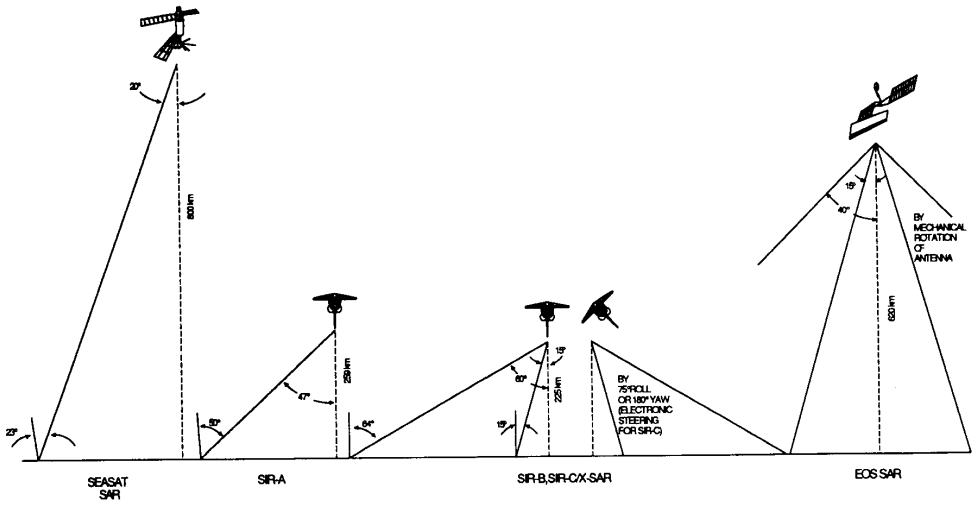

Fig. 3. The altitude and look/incidence angle coverage for the Seasat SAR, SIR-A, SIR-B, SIR-C/X-SAR, and the EOS SAR.

3-day near repeat, and the orbit for the remainder of the mission was a 3-day exactly repeating orbit. A total of 100 million square kilometers of the Earth were imaged by the Seasat SAR (Fig. 4).

B. SIR-A

The success of the Seasat SAR prompted the first flight of a SAR on the shuttle. The shuttle was seen as an op-

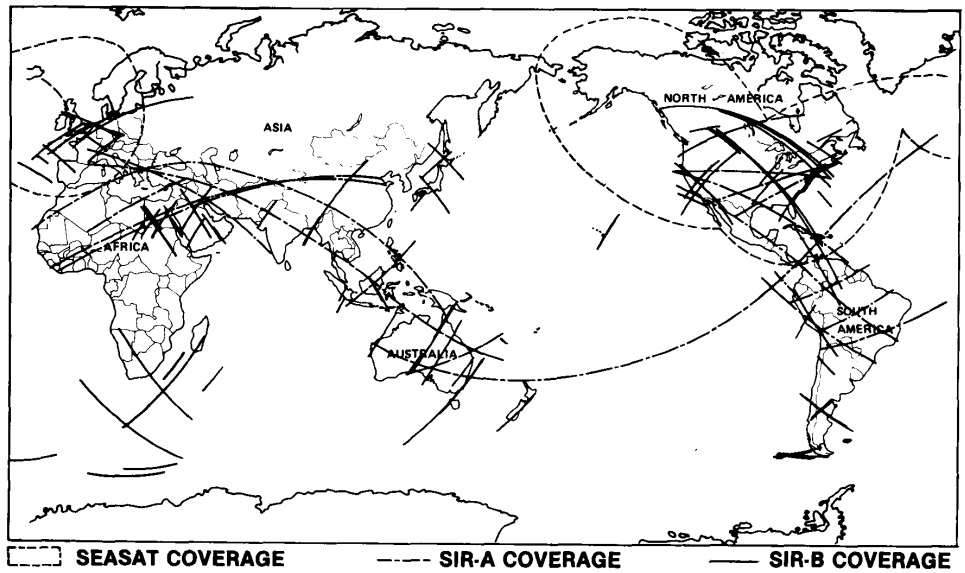

Fig. 4. Coverage for the Seasat SAR, SIR-A, and SIR-B.

portunity to progressively develop and fly increasingly more complex imaging radars for short missions, allowing the hardware to be returned to Earth for reuse on follow-on missions.

1. Instrument. The system characteristics for the first Shuttle Imaging Radar, SIR-A, were defined primarily by the spare parts available from the Seasat SAR (Fig. 5). SIR-A, therefore, had essentially the same design as Seasat (Table II, Fig. 1(b)): L-band wavelength and HH polarization [19], [20]. The antenna look angle was fixed at 47° in order to optimize geologic mapping in topographically rough terrain. SIR-A required no more power than Seasat (1 kW) to image at the larger look angle because of the lower shuttle altitude of 259 km and the higher expected backscatter of geologic surfaces relative to the ocean's surface. Although there were preflight plans to point the SIR-A antenna at different incidence angles by rolling the entire shuttle, these plans were deleted when problems occurred during the flight. From the shuttle altitude, the 2.16-m antenna width (spare Seasat SAR antenna panels were used) provided a 50-km swath at the 50° incidence angle. Eight antenna panels were used; one fewer than required for Seasat, again because of the lower altitude, resulting in a 9.4-m antenna length. The antenna was mounted in a fixed open position on the starboard side of the payload bay with the long axis parallel to the velocity vector when the shuttle was flying nose forward, allowing imaging only on the northern side of the shuttle nadir track.

The optical recorder on which the data for SIR-A were recorded was a spare from the Apollo 17 Lunar Sounder Experiment and was 14 years old when it was flown on SIR-A. It limited the resolution to 40 by 40 m (4 looks). The bandwidth was accordingly selected to be 6 MHz. Because the data were collected and processed optically, it was not possible to calibrate the SIR-A radar.

SIR-A provided much improved image data for geologic analyses as they were relatively free of the layover distortion that accompanied Seasat images in high-relief regions [19], [21], [22]. SIR-A also led to the discovery of buried and previously uncharted dry river beds beneath the Sahara Desert in Sudan and Egypt [23]–[25]. This demonstrated the ability of an L-band radar to penetrate up to several meters in hyperarid sand sheets.

2. Data system. Because simplicity was a requirement for SIR-A, the data were recorded optically in the payload bay and were not accessed until the film was off-loaded after landing (Fig. 2). Optical recording and processing limit the resolution, dynamic range, and calibration potential and are therefore not desirable; however, optical recording has thus far proven to be a very reliable method for collecting SAR data on the shuttle and provides a data set that can be processed quickly and inexpensively.

3. Mission design. SIR-A was launched on November 12, 1981 into a 38° inclination orbit at a 257-km altitude on the second shuttle flight (STS-2 on Columbia) and the first to carry a scientific payload (OSTA-1) (Fig. 3). Due to difficulties which occurred during the flight, the mission lasted only 2 days. The total global coverage is shown in Fig. 4; 10 million square kilometers of the Earth's surface were imaged.

C. SIR-B

With the success of SIR-A, the radar was upgraded significantly. SIR-B, the follow-on to SIR-A, had the addi-

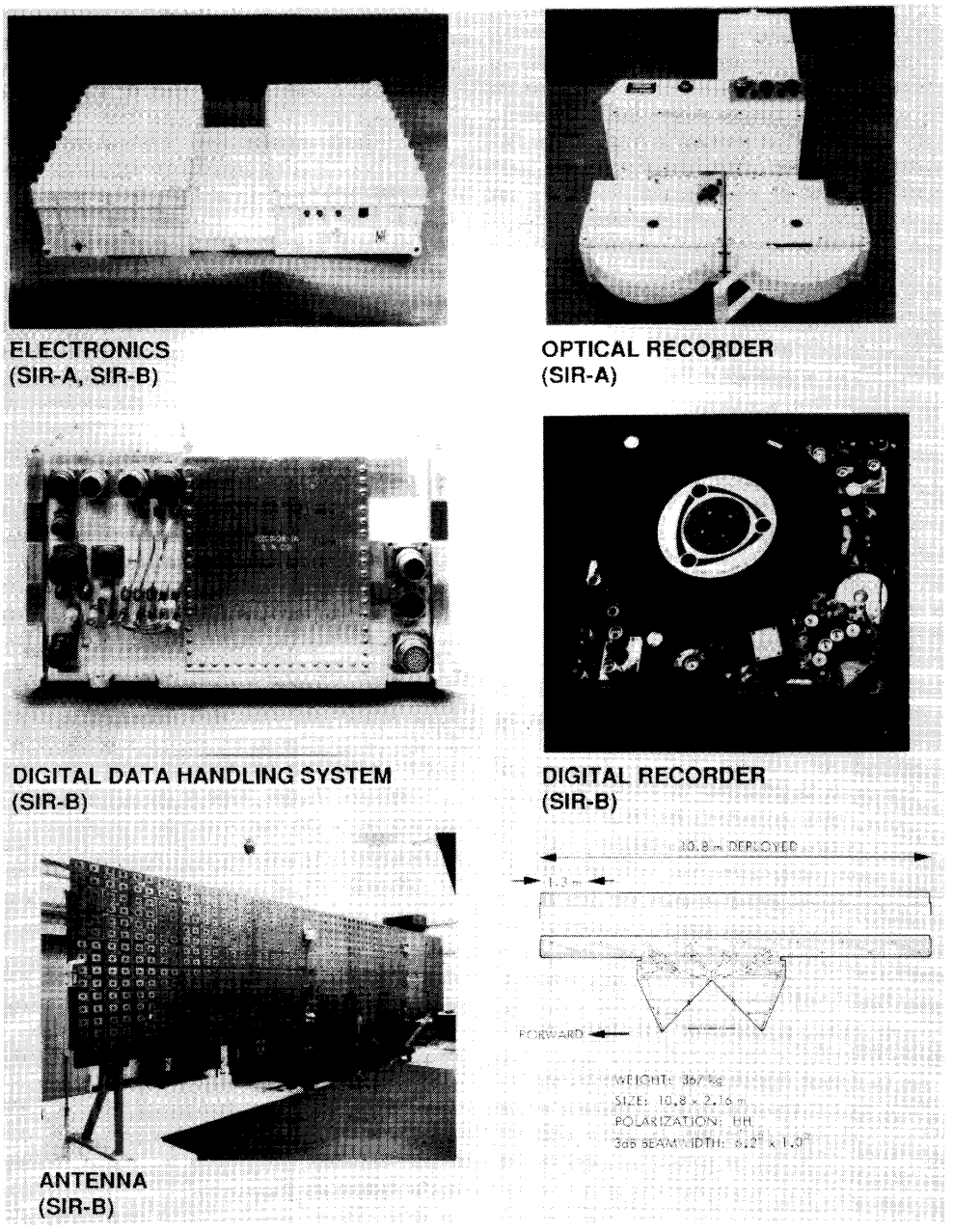

Fig. 5. Shuttle Imaging Radar hardware.

tional flexibility of imaging geometry, particularly the effect of incidence angle on radar backscatter [26]–[30].

1. Instrument. The L-band system was left essentially intact for SIR-B (HH polarization and 1 kW power), but the antenna panels were mounted on a new support structure which allowed them to be mechanically tilted to any look angle between 15 and 60° (Fig. 1(c)). Thus, other nadir-looking instruments flying with SIR-B could continue to operate from a fixed "payload bay to Earth" shuttle attitude as the radar acquired multiincidence angle data. The beamwidth of SIR-B was constant, thus the illuminated swath on the ground was determined by the look angle. At low look angles, the maximum swath was the beam-limited swath. One additional panel was added to the SIR-B antenna to extend its ambiguity limit at high look angles bringing its total length to 10.7 m. Again, the

antenna was mounted on the starboard side of the payload bay with the long axis parallel to the velocity vector when the shuttle was flying nose forward, allowing imaging on the northern side of the shuttle nadir track. The southern side of the track was also imaged during the SIR-B flight by rolling the shuttle 75° or yawing it 180°. Other imaging geometries, including squint, spotlight, and a 360° yaw, were accomplished by pitching and yawing the entire shuttle. Squinting is particularly desirable to determine the azimuthal angle dependence of the backscatter which may be used to discriminate surface structure, and to provide a variety of viewing angles in topographically complex regions. The spotlight mode provides improved radiometric resolution by reducing the speckle through incoherent averaging of a data set collected over a longer period of time. These data, and those collected in the 360° yaw mode, can also be processed to provide several near simultaneous data sets acquired at different azimuth angles over a single target, a technique which can be used to assess the multiangle character of rapidly varying ocean waves, for example. Due to power limitations resulting from the failed SIR-B antenna, none of the data collected in these various imaging geometries provided useful imagery; only the ability to accomplish the shuttle maneuvers to acquire the data was demonstrated. A final improvement to the antenna was the ability to fold for launch in order to accommodate additional deployable payload. SIR-B was folded in two places along its length making its folded dimensions 2.16 m × 3.6 m.

With the addition of a digital data handling system (DDHS) on SIR-B, it was feasible to double the bandwidth to 12 MHz, thus improving the resolution over SIR-A by a factor of two (at the 50° incidence angle). At high incidence angles where the resolution is increasingly finer, the collected swath was less than the illuminated swath to fit within data rate limitations. In order to add some flexibility to this limitation, it was possible to select the number of bits per sample (6, 5, 4, or 3 bps) to collect a wider swath. The digital data system also made calibration possible; therefore, a calibrator was added to the electronics which supplied a known reference signal. The addition of the calibrator was critical to experiments designed to determine the backscatter vs. incidence angle characteristics of various terrain types, as data at each incidence angle were collected on successive days of the mission [31]. Forty-three principal investigators were involved in the SIR-B experiment; their experiment objectives are summarized [26]. Key results of the SIR-B mission are described [28]–[30], [32]–[34].

2. Data system. The first imaging radar system with digital recording to fly on the shuttle was SIR-B (Fig. 2). A digital data handling assembly (DDHA) converted the analog signal to a digital signal onboard the shuttle. This digital signal was then sent through the shuttle Ku-band antenna to the Tracking and Data Relay Satellite (TDRS), then to White Sands. From there the data were sent to Goddard Space Flight Center (GSFC) via the Domsat communication satellite where they were recorded and shipped via airplane to the Jet Propulsion Laboratory (JPL) for processing. There were two data rate bottlenecks of equal size in the radar to Goddard link: the Ku-band antenna and Domsat, both of which are limited to 50 Mbps.

The SIR-B mission flew when there was only one TDRS, thus limiting acquisition and direct down-linking of digital data to North and South America, Europe, and Africa. This constraint was overcome by adding a high data rate tape recorder (30 Mbps) and seven 20-min high density tapes in the crew aft flight deck. Data could then be recorded and later played back through TDRS or offloaded on one of the available tapes. The data sent directly through TDRS and those collected on the recorder were of equal quality; however, because of the reduced data rate, the data collected on the recorder had a 1/3 narrower swath width.

During the first data acquisition for SIR-B, the Ku-band antenna failed, thus preventing the use of the direct data downlink through TDRS for the remainder of the flight. In-flight repairs by the shuttle crew allowed transmission of data through the antenna, but it could not be rotated to track TDRS. Thus, all SIR-B data were collected on the onboard digital recorder and later dumped through TDRS by maneuvering the entire shuttle in order to track the TDRS satellite.

Most of the SIR-B processing was done post flight [18]. Some of the data were also processed in near real time during the mission as an engineering check of the data quality. All SIR-B data have been digitally processed.

3. Mission design. One of the advantages of flying an instrument on the shuttle is that it is possible to select a very specific orbit designed to accomplish the Earth observing goals of one or a few instruments. SIR-B was launched on October 5, 1984, on Challenger, (279:11:03:00 GMT) into a 57° inclination orbit, the maximum possible from Kennedy Space Center, to a final altitude of 224 km (Fig. 3). With this orbit, a slow drift of about 1° per day at the equator allowed multiple angle imaging on successive days of the mission. With the slowly drifting orbit, only a portion of the Earth could be accessed, therefore the first 2 days of the mission were flown at two different altitudes of 354 km (orbits 1–22) and 257 km (orbits 23–33) thus providing access to all targets between ±60° latitude. Again, difficulties occurred during the flight which limited the volume of digital data collected and decreased the planned multiple angle coverage significantly. Approximately 7 million square kilometers of digital data were acquired and approximately 15 multiple angle (two or more angles) data sets were obtained (Fig. 4).

D. SIR-C/X-SAR

SIR-C/X-SAR will take a major leap toward the final EOS design [35]–[37a] by adding polarimetric multifrequency imaging.

1. Instrument. A multipolarization, active phased array C-band system will be added for SIR-C and a more

powerful multipolarization active phased array L-band system will replace the 1 kW HH polarized passive array that has flown since Seasat (Fig. 1(d)). Instead of using a single, high power transmitter, the SIR-C SAR antennas will contain numerous low power solid state transmitters distributed across the antenna aperture. Large power losses which typically occur in the corporate feed of the conventional passive antennas will be avoided and as much as an eight-fold improvement in efficiency will be possible. In addition, the inherent redundancy and the extended lifetime of the distributed systems make them more desirable for the long duration EOS mission. The active phased array C- and L-band SIR-C SARs will allow electronic beam steering in the range direction ($\pm 23°$) from a fixed antenna position of 38° (look angle), thus making it possible to acquire multiincidence angle data without tilting the entire antenna. In order to acquire high quality cross-polarized data at high incidence angles, the peak power for the C-band system is 2.2 kW and that for the L-band system is 3.5 kW.

An X-band radar built jointly by the Deutsche Forschungsanstalt für Luft-und Raumfahrt (DLR) in Germany and the Agenzia Spaziale Italiana (ASI) in Italy, called X-SAR, will fly with SIR-C [38]–[41]. Because of limitations in the available technology at that frequency, the X-band SAR will only have VV polarization and no scanning capability. X-SAR is a follow-on to the European Microwave Remote Sensing Experiment (MRSE) which flew aboard Spacelab in December, 1983. MRSE was also an X-band SAR, although with a reflector antenna instead of a passive array like X-SAR. Although the MRSE experiment was not successful only as a radiometer and not as a SAR it did provide experience for the X-SAR instrument.

The total dimensions of the SIR-C/X-SAR antenna are 4.1 m × 12 m. This allows for a 2.9-m wide L-band antenna (2 rows of 1.3 m panels), a 0.75-m wide C-band antenna (1 row of .7 m panels), and a 0.4-m wide X-band antenna. As SIR-C/X-SAR is a dedicated payload only the Mapping of Air Pollution from Space (MAPS) instrument will fly in the payload bay with the radar, there is no requirement to fold the antenna for launch. The SIR-C/X-SAR antenna will be mounted flat for launch with its upper and lower edges resting on either side of the pallet. Once in orbit, the antenna will be tilted and the shuttle rolled to a nominal 38° look angle. In order to acquire data at look angles other than 38° with the conventional X-band system, the X-band antenna, which is mounted along the upper portion of the array, may be mechanically tilted to any look angle between 15 and 60°. As with SIR-B, data may be acquired on either side of the shuttle nadir track by rolling or yawing the shuttle. Imaging in the squint mode may also be accomplished by maneuvering the entire shuttle; however, the spotlight mode data may be acquired electronically. Swath widths for SIR-C/X-SAR will be limited primarily by the available data rate and will depend on the number of bands collected on a given pass; in general they will be between 15 and 90 km. Wider swaths may be acquired in an experimental 3-beam scanSAR mode in which data are acquired in three parallel swaths nearly simultaneously by electronically scanning in three steps on a pulse-by-pulse basis.

The present SIR-C/X-SAR design includes bandwidths of 10, 20, and 40 MHz with the 40-MHz bandwidth providing better resolution than that available on SIR-B. The 10-MHz bandwidth has been added for a low resolution mode in order to increase the swath for a given available data rate.

SIR-C/X-SAR is scheduled for three flights in three different seasons on the Space Radar Laboratory (SRL) in order to study seasonal change in ecosystems, oceans, and snow and soil moisture. It will therefore be essential to obtain absolute calibration of the SIR-C/X-SAR system for data comparisons between the three flights. Details of the calibration plan are presently under consideration; however, the goal is to obtain ± 1 dB relative calibration and ± 3 dB absolute calibration. The techniques used to obtain these high levels of calibration will include preflight calibration, in-flight internal calibration (including frequent onboard measurements of transmitted and received power levels), and in-flight overall system calibration using artificial ground targets with known scattering properties.

2. Data System. The SIR-C/X-SAR data system will be substantially more advanced than the SIR-B system in order to handle the multipolarization modes (Fig. 6). In the quad-pole mode, the H and V transmitters operate on alternate transmitted pulses. The H and V receivers both receive all return pulses, half of which are horizontally transmitted and half of which are vertically transmitted. This procedure requires twice the pulse repetition frequency (PRF) of a single polarization mode. If both the L- and C-band channels are operated simultaneously, four 45-Mbps data streams will allow acquisition of all eight channels simultaneously with about a 30-km swath. This scenario requires four digital data handling assemblies (DDHAs) and a data steering network (Fig. 2). The data collected on the recorders may be stored onboard on high density tapes or dumped through TDRS for engineering checks. The primary mode of data storage for SIR-C/X-SAR will be on the onboard recorders on tape cassettes. Only selected data will be transmitted through TDRS to the ground for real-time analysis. The SIR-C radars will use two recorders and X-SAR will use a third recorder.

Processing for the SIR-C L- and C-band data will be done at JPL using a super minicomputer which is capable of processing at a rate of 1/5 real-time for survey data (a 10 s data take would take 50 s to process), and 1/100 real-time for standard data. X-SAR data will be processed at DLR and ASI. Coregistration of the two data sets must be done using tie point techniques, although it may be possible to process SIR-C and X-SAR data together at JPL in order to obtain automatically coregistered data sets.

3. Mission Design. Presently SIR-C/X-SAR is scheduled for three launches 6 to 18 months apart in the mid 1990s. The current manifest schedules the first flight for

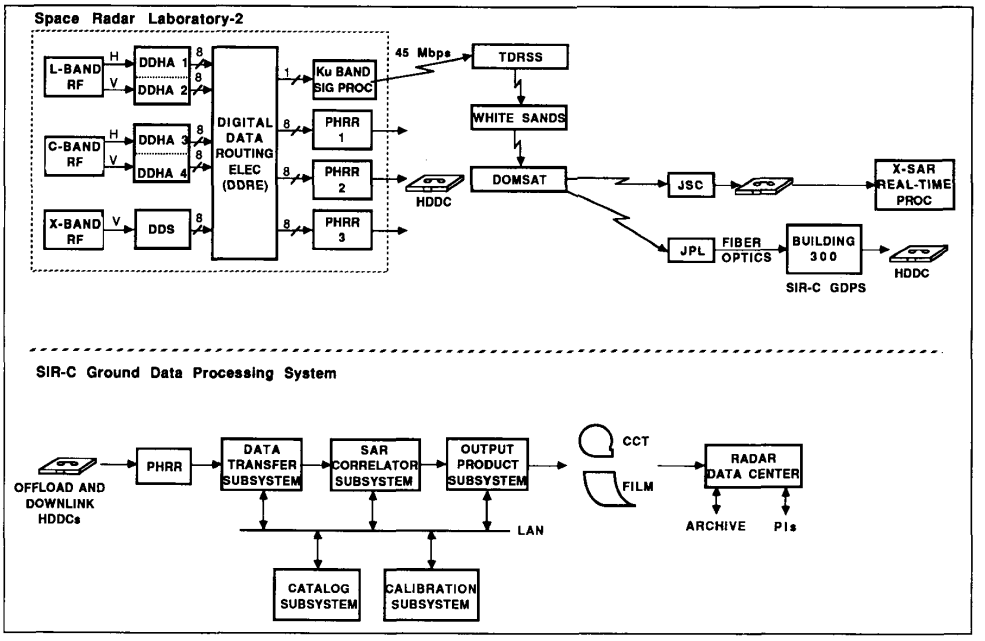

Fig. 6. End-to-end data flow for the SIR-C/X-SAR system.

July, 1993, the second for October 1994, and the third for May, 1996. The inclination will be 57° to provide the maximum latitudinal coverage available from a Cape Kennedy launch. The altitude for the SIR-C/X-SAR flights has not been finalized at this time but it will most likely be about the same as SIR-B in order to again provide multiple incidence angle imagery.

III. Aircraft Radars

Spaceborne SARs provide extensive coverage with little variation in incidence angle across a wide swath and are therefore preferred as a source of microwave data for long-term studies. Aircraft SARs are, however, essential for developing algorithms using specific test sites and for obtaining data with a variety of imaging geometries and temporal coverage patterns. Today there are many research aircraft SARs available, four are described here: the NASA/JPL Aircraft SAR (AIRSAR) mounted on NASA's DC-8, the P-3 SAR System mounted on a Navy Orion P-3 aircraft, operated by the Naval Air Development Center (NADC); the Canadian SAR, operated on a CV-580; and the DLR Aircraft SAR (Table III). These aircraft systems will eventually be used for long-term calibration as they will provide a calibrated link or reference between the spaceborne missions. Other airborne SAR systems include the STAR-1, IRIS, CASSAR, KRAS, and the VARAN-S.

A. AIRSAR

1. Instrument. From 1970 through 1984, NASA operated an L-band, and in 1984 added a C-band multipolarization airborne SAR system on NASA's CV-990 research aircraft [43], (Fig. 7(a)). This system, along with the CV-990, was lost in an aircraft fire in July, 1985. Funds were immediately set aside to rebuild the SAR and purchase a new aircraft, this time a DC-8. The system designated as AIRSAR was used as a basis for the SIR-C and EOS SAR designs in frequency (L- and C-bands) and polarization [44]. The antennas are H/V microstrip antennas. The resolution of the aircraft system is approximately 10 m (3.75 m slant range) with a swath width of either 7 km (40 MHz bandwidth) or 13 km (20 MHz). Incidence angles range from about 20 to 60°, and data are acquired from the port side of the aircraft. In addition to the L- and C-band SARs, a P-band (67 cm) system was also added along with a second L- and C-band antenna towards the front of the aircraft to allow collection of interferometric data. The AIRSAR operates in several special modes including the along-track interferometer to study surface motion (L- and C-bands, dual polarization) and a new cross-track interferometer to measure topography (C-band).

2. Data system. The airborne SAR data are recorded digitally onboard the aircraft on three High Density Digital Recorders (HDDRs). All eight channels (where a channel is single frequency and single polarization) may be recorded on a single recorder with a tape capacity of 15 min; the data rate is 10 Mbps. Data may be processed onboard in a quick-look frame mode or using the real time processor which possesses a full swath, single channel with 2 looks and 25–30 m resolution. At JPL, the data may be processed in the full resolution 12-channel, 4-look

TABLE III
AIRCRAFT SARs

	NASA/JPL	P-3 SAR	CCRS C/X-SAR	DLR SAR
Imaging Characteristics				
Band (wavelength, cm; frequency, GHz)	L (23.9, 1.25) C (5.6, 5.3) P (67, 0.438)	L (23.9, 1.25) C (5.7, 5.3) X (3.2, 9.34)	C (5.66, 5.30) X (3.24, 9.25)	L,C,X
Polarization	quad	quad	quad	HH,VV
Look Angle (deg)	20–60°	11–79°	0–74°, 45–76°, 45–85°*	
Azimuth Resolution (m)	2	2.2	6, 6, 10*	3
Range Resolution (m)	7.5 (slant range)	8.4	6, 6, 20*	3
Looks	4	4	7	8
Swath (km)	7–13	6–48	22, 18, 63*	3
Instrument Characteristics				
Peak Power (kW)	1		3.4 (C), 3.8 (X)	
Bandwidths (Mhz)	20, 40		25, 8 (C); 31, 7.5 (X)	
Antenna Width × Length (cm)	91.4 × 182.9 (P) 45.7 × 161.3 (L) 16.5 × 135.9 (C)			
Aircraft Characteristics				
Altitude (km)	8	3–8	5–6	
Flight Duration	8–11 h	8–12 h	5 h	
Aircraft	NASA DC-8	NADC P-3	Convair-580	DO 228
Operational Date	1988	1988	1978	1989
Data Characteristics				
Simultaneous Channels**	12	4	1 (2 if half swath)	1
Recorder Capacity/HDDT (min)	15	20		
Processing				
Type	digital	digital	digital	digital
Location	JPL	ERIM	CCRS	DLR
Real Time	yes (image, strip)	yes (strip)	yes (2 strips/X and C)	yes

*nadir mode, narrow swath mode, wide swath mode.
**one channel = single frequency, single polarization.

single scene mode, or using survey processing, a full resolution 16-look, three-channel mode with a swath of 8.5 × 60 km. The aircraft began operating in January, 1988 with its first scientific deployment to Alaska in March, 1988 for ice, snow, forestry, and permafrost penetration investigations.

B. P-3 SAR System

1. Instrument. A few months before the NASA/JPL aircraft SAR began flying, the NADC P-3 SAR System began its initial calibration and checkout flights. Its first science mission was also to Alaska in March, 1988 when, for the first time, the NASA/JPL and P-3 aircraft SARs collected data nearly simultaneously over both ice and forests allowing cross-calibrated using the same ground calibration equipment.

The P-3 SAR (Fig. 7(b)) also duplicates the SIR-C/X-SAR and EOS SARs because it is a full polarization system which can operate at X-, C-, and L-bands [46]. In its wide bandwidth (120 MHz) mode, the P-3 SAR System has a 1.2-m (range) by 2.1-m (azimuth) resolution with a 4.9-km slant range swath width. In its narrow bandwidth mode (60 MHz), this SAR has 2.4-m (range) by 2.1-m (azimuth) resolution and a 9.8-km slant range swath width. The ground range coverage of the system is dependent upon both the incidence angle coverage (which is selectable from 0 to 85°), and the aircraft altitude (which is selectable between 3 and 8 km).

2. Data system. The P-3 SAR System records data on a single high density tape recorder. Because of the presumming required before processing, as well as the sheer volume of data, only four of the 12 channels of SAR imagery are recorded during the same pass (even so, one HDDT is filled for every 20 min of data collection). The system can record the four polarization channels from a single frequency, any frequency/polarization combination, or wider swaths of a limited number of frequency/polarizations. The system also has an onboard real-time processor which allows review of the data-take several seconds after a region is imaged. This real-time processor is limited to a single channel of data which may be any frequency/polarization combination.

C. Canadian Aircraft SAR

1. Instrument. The Canadian Centre for Remote Sensing (CCRS) CV-580 aircraft SAR system [47]–[49] has been operational since 1978, originally in cooperation with ERIM. Since 1986, hardware has been developed in Canada. Currently, both C- and X-band SARs are flown (Fig. 7(c)) and the CCRS aircraft SAR has participated in many national and international remote sensing campaigns.

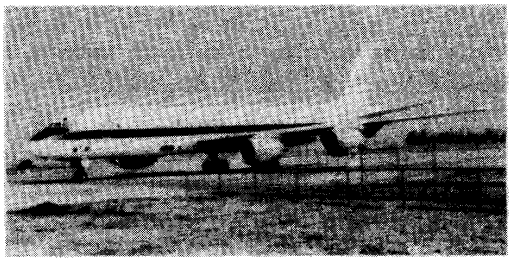

(a)

(b)

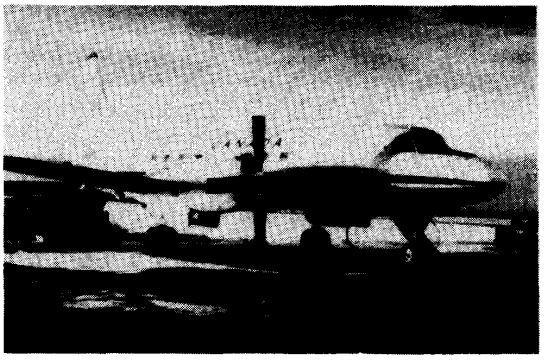

(c)

Fig. 7. Three of the airborne SAR platforms including (a) NASA/JPL which flies on the Ames DC-8, (b) NADC/ERIM SAR which flies on the NAVY P-3, and (c) the CCRS SAR which flies on a CV-580.

The SAR collects data in two resolution modes: 6 × 6 m (high resolution) or 10 × 20 m (asimuth x range; low resolution). Variable swath width and geometry is possible in three modes: nadir mode (0–74°; 22 km swath), narrow swath mode (45–73° look angle, 18 km swath) and wide swath mode (45–85° look angle, 63 km swath; low resolution only). Each SAR has two receivers and dual polarized antennas so that reception of both like and cross-polarized is possible. However, in order to record real-time processed data from both channels, the swath width is reduced in half. A fast ferrite switch is being incorporated into the C-band SAR to convert it into a full polarimetric radar and an additional receiving antenna has been mounted on the side of the Conviar to create an interferometric SAR for terrain elevation mapping

2. Data System. Both image and signal data (range compressed but not azimuth compressed) are recorded on separate HDDTs, one for signal data for each frequency and a third for the real-time imagery. The signal data can be transcribed to CCT on the ground and processed on a variety of SAR processors. Also, image data is transcribed to CCT and provided to users as hard copy or in digital form.

The DLR Aircraft SAR [43] is an experimental system operating at L-, C- and X-band, one channel at a time. Each band may be operated at VV or HH polarization. A polarization-switching capability from pulse to pulse will be available in the fall of 1991, while quad pol operation is planned for 1993 in C-band. The SAR is mounted in a small twin engined propeller aircraft DO 228. Its normal mode produces 8-look images of 3 × 3 km and a resolution of 3 × 3 m.

Data collected with the DLR SAR are stored on HDDT for subsequent processing on the ground. The transcription uses video cassettes, which are also used as data input for the image processor. Presently, an unfocused quick-look procedure is used for real time processing onboard. It will be replaced by a hardware processor which has the full high precision capability. Radiometric calibration experiments have been successfully carried out with this SAR system [50.2].

IV. International Spaceborne Imaging Radars

The year 1991 may mark the beginning of a permanent presence in space of synthetic aperture radars. Starting with the Soviet Union's Almaz-1 launched in March 1991 followed by the European's first ESA Remote Sensing (ERS-1) satellite launched in July 1991, a continuous radar data set will be available potentially through the end of the EOS era, if all missions fly as currently scheduled. The Almaz-1 and ERS-1 missions will be followed by the Japanese Earth Resources Satellite (JERS-1) scheduled for a 1992 launch, followed by RADARSAT which has a current design life of 5 years and is set for launch in 1994. Each of these missions is unique in its choice of frequency, polarization, resolution, swath width, repeat interval, orbit altitude and inclination, and data acquisition scenario (Table IV); however, with proper calibration, the missions may be used together to obtain an extended data set in the active microwave frequency region.

A. Almaz-1

1. Instrument. On March 31, 1991, the Soviet Union launched a spaceborne SAR called Almaz-1; almaz means diamond in Russian. Almaz-1 was preceded by Cosmos-1870 which was launched in July 1987; this mission lasted 2 years. The Almaz-1 SAR was launched on a Proton booster from the Soviet Union's Baikonur Cosmodrome. Almaz-1 is a single frequency S-band (10-cm wavelength), single polarization SAR with a spatial resolution of 15 to 30 m, depending on the incidence angle, and a swath width of 20 km. Incidence angles are selectable between 30 and 60°. There are two slotted waveguide scan-

TABLE IV
THE INTERNATIONAL SPACEBORNE MISSIONS

	Almaz-1	ERS-1	JERS-1	RADARSAT
Imaging Characteristics				
Band (wavelength (cm), frequency (GHz))	S (10, 3.0)	C(5.7, 5.25)	L(23.5, 1.275)	C(5.7, 5.3)
Polarization	HH	VV	HH	HH
Look (Incidence) Angle	30°-60°	20°(23°)	35° (38°)	(20°-59°)
Swath (km)	20-45	100	75	45-500
Range Resolution (m)	15-30	20	18	10-100
Azimuth Resolution (m)	15	30	18	10-100
Looks		4	3	1-16
Right/Left Looking	both	right	right**	right***
Instrument Characteristics				
Antenna Type	waveguide	corporate feed	corporate feed	phased array
Antenna Size (mxm)	15 × 1.5 (two)	10 × 1	11.9 × 2.4	15 × 1.5
DC Power (W)		1245	675 (1100 peak)	300 (5000 peak)
Bandwidth (MHz)		15.5	15	30, 17.3, 11.6
Noise Equivalent σ°		−18	−20.5	−23
Orbit Characteristics				
Altitude (km)	300	785, 782	568	793-821
Inclination	73°	98.5°	97.7°	98.6°
Sun Synchronous?	no	yes	yes	yes
Equator Crossing Time	—	10:30 a.m.	10:30-11:00 a.m.	6:00 p.m.
Daytime Node	—	descending	descending	terminator
Exact Repeat Cycle (days)		3, 35, 176	44	24
Approximate Repeat Cycle				
Mission				
Spacecraft	Almaz-1	ERS-1	JERS-1	RADARSAT
Launch Date	March 31, 1991	July 16, 1991	February, 1992	December, 1994
Mission Duration	2 years	2-3 years	2 years	5 years
Data Characteristics				
Downlink Data Rate (Mbps)		105	30 (2 channels)	74-105
Downlink	recorder/ ground station	ground station	recorder/ ground station	two recorders/ ground station
Recorder Rate (Mbps)		—	32 × 2 channels	85
Recorder Capacity (min)	2	—	20	10
Operation Time/Orbit		10 min	20 min	28 min
Processing				
Type	digital	digital	digital	digital
Location	USSR	ASF, Canada, Europe, etc.	ASF, Canada, Europe, Japan, etc.	ASF, Canada, Europe, etc.
Other Sensors				
	Radiometric Scanner (RMS)	Radar Altimeter, Wind/Wave Scatterometer, Along Track Scanning Radiometer	Optical Sensor (OPS)	None

**yaw 180° to map Antarctica
***two 2-week periods with SAR left looking are planned

ning antennas each 15 × 1.5 m in size, one on each side of the spacecraft providing imaging on either side of nadir.

2. Data system. Data may be stored on onboard recorders with 150 s of recording time. Almaz data products are available commercially through a joint agreement between Glackosmos (USSR) and Space Commerce Corporation (SCC, US) ("Buyers Guide, Almaz Remote Sensing Satellite", 1990).

3. Mission design. The Almaz-1 orbit altitude is 300 km with an orbit inclination of 73°. A sounding radiometric scanner (RMS) system and several infrared bands are also on the spacecraft. The planned lifetime of Almaz-1 is 2 years with a second launch scheduled for 1993.

B. ERS-1

The second of the long-duration spaceborne SAR systems is the European Space Agency (ESA) Remote Sensing (ERS-1) satellite (Duchossois, 1986). ERS-1 was launched from the Guyana Space Center on an Ariane 4 on July 16, 1991 (1991:198:01:46) for a 2-year nominal mission (Fig. 8(a)). The mission is primarily oriented toward ice and ocean monitoring; however, a variety of other applications are included in the nearly 200 investigations which were approved by ESA.

1. Instrument. The ERS-1 SAR is part of the Advanced Microwave Information (AMI) package, a unit with shared electronics for the SAR and a scatterometer

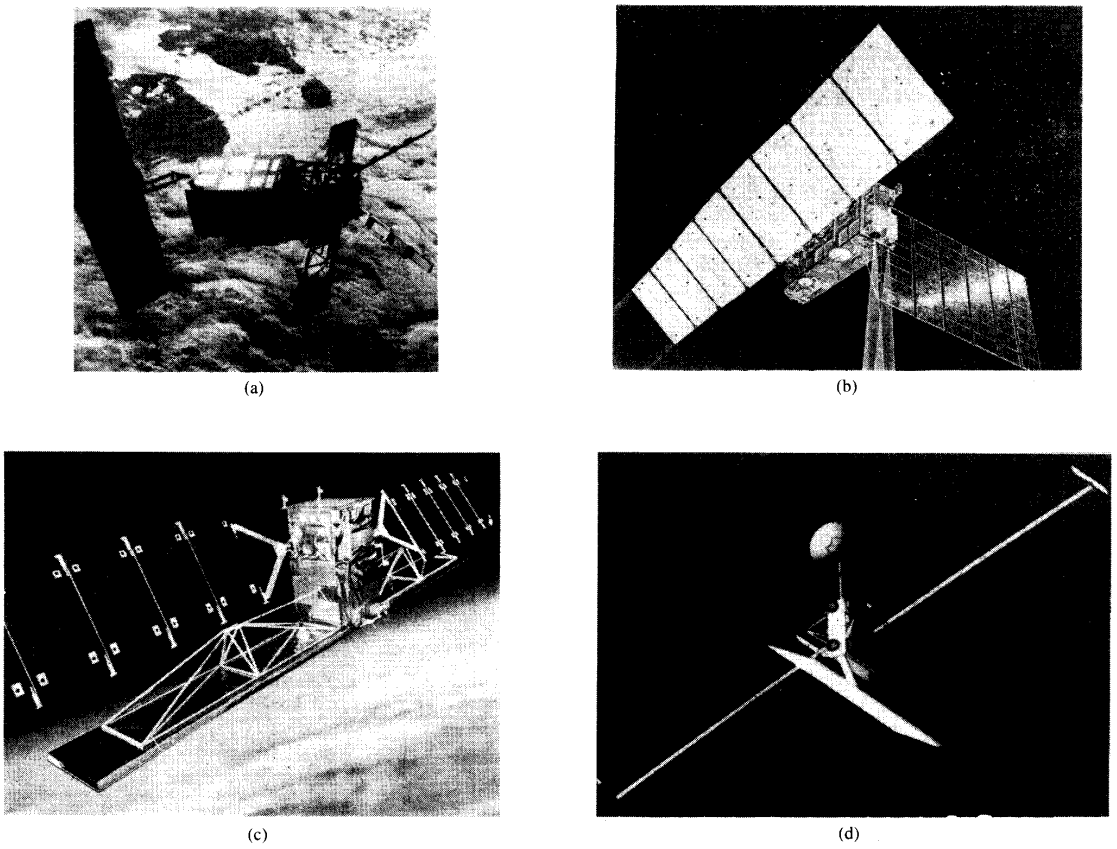

Fig. 8. The international spaceborne missions including (a) ERS-1, (b) JERS-1, and (c) RADARSAT. Also shown in the EOS SAR (d). The RADARSAT image was provided by Ball Aerospace Systems Group.

which can be operated in either a wind or a wave mode. As a result, the operation of the SAR and scatterometer are mutually exclusive. The C-band SAR has VV polarization and an incidence angle of 23°. The swath width is 100 km with 30 m resolution at 4 looks. The 10 × 1 m SAR antenna is mounted on the right side of the spacecraft.

2. *Data system.* Data from ERS-1 is transmitted to a number of ground receiving stations (Fig. 9) including the NASA-funded Alaska SAR Facility (ASF) built at the University of Alaska's Geophysical Institute in Fairbanks [53]–[55]. ESA stations for ERS-1 include Kiruna (Sweden), Fucino (Italy), Maspalomas (Canary Islands, West Africa), and Gatineau and Prince Albert (Canada). Other stations include Tromsoe (Norway), West Freugh (Scotland), Aussagel (France), Hyderasad (India), Pari Pari (Indonesia), Alice Springs (Australia), Cotopaxi (Equador), Cuiaba (Brazil), Matoyama and Kumamoto (Japan), Bangkok (Thailand), and Syowa and O'Higgins (Antarctica), funded by Japan and Germany, respectively, as well as other locations currently in either the planning or construction stage. No onboard recording capability is included; therefore, only regions in view of the ground receiving stations are accessible to ERS-1. The high rate SAR data is transmitted at 105 Mbps.

3. *Mission design.* ERS-1 is in a sun-synchronous orbit of 97.5° inclination and an initial altitude for the Commissioning Phase (first 3 months) of 775 km. This altitude is being used to define the calibration parameters of ERS-1 and is an exact 3-day repeat. After the Commissioning Phase, ERS-1 will be moved to a second 3-day repeat with a node optimized for the polar regions called the First Ice Phase starting January 1, 1992. After the 3-month Ice Phase, the orbit will move to a Multi-Disciplinary 35-Day Repeat until December 15, 1993. A Second Ice Phase, again with a 3-day repeat, and a Geodetic Phase with a 176-day repeat will follow.

Other instruments to fly with ERS-1 include a Radar Altimeter (RA; Ku-band, 13.7 GHz), and an Along-Track Scanning Radiometer (ATSR), as well as a Precise Range and Range Rate Equipment (PRARE) and a Laser Retroreflector (LRR) for determination of the satellite position.

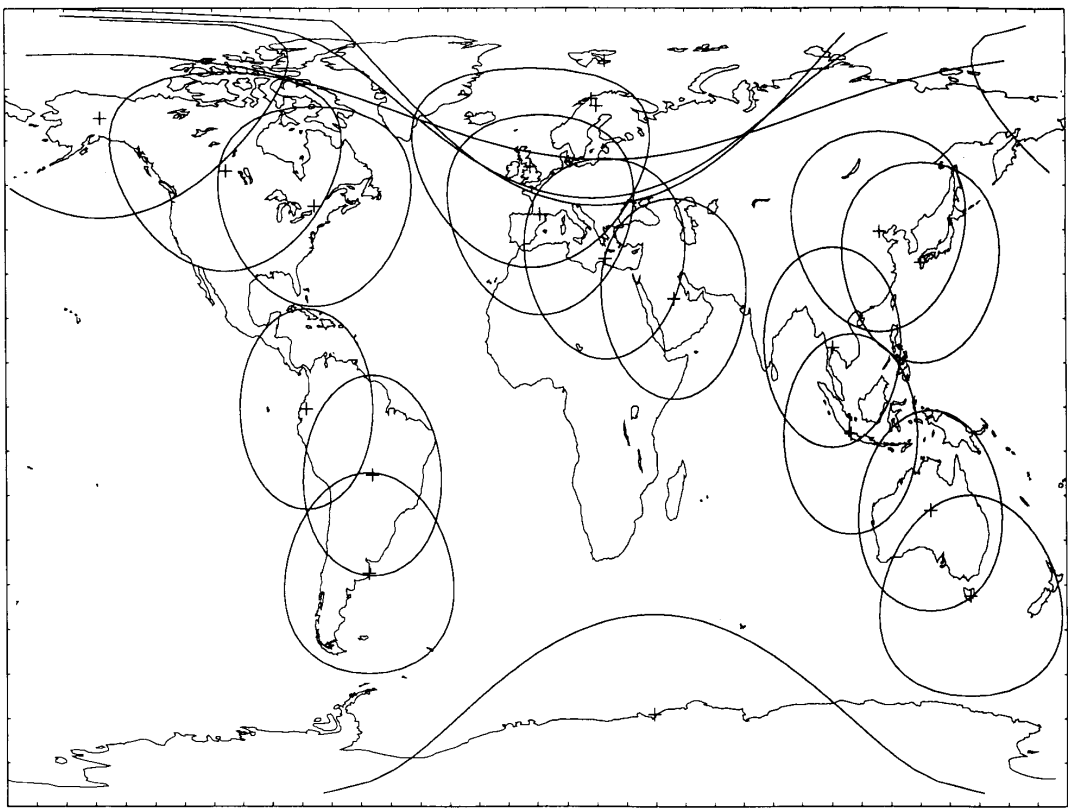

Fig. 9. Ground receiving station coverage for the planned stations for ERS-1, JERS-1, and RADARSAT.

ERS-1 may be followed by ERS-2, a copy of the ERS-1 SAR, thus extending the C-VV data set by 2 to 3 years.

C. JERS-1

In early 1992, National Space Development Agency (NASDA) and the Ministry of International Trade and Industry (MITI) of Japan will launch the first Japanese Earth Resources Satellite (JERS-1) on the H-1 rocket from Tanegashima Space Center in Japan (Fig. 8(b)). Specifically, MITI is developing the instrument and NASDA is developing the spacecraft bus and handling the launch and operations. The primary scientific objectives of the JERS-1 mission are to establish an integrated system of optical and microwave sensors for examining the terrestrial resources and environment, focusing on geological and topographic surveys. Specific applications include land research, agriculture, forestry and fisheries, environmental preservation, disaster prevention, and coastal monitoring. In addition to the SAR, JERS-1 will carry an optical sensor (OPS) with seven bands (0.52–0.6, 0.63–0.69, 0.76–0.87, 1.62–1.71, 2.01–2.12, 2.13–2.27, and 2.27–2.40 μ) and one additional band at 0.76–0.87 μ which will be used to acquire data at a 15° look angle in the forward direction to provide stereo imaging. The 75 km swath, 18 by 24 m resolution OPS system will provide a complimentary yet not simultaneous data set to the SAR.

1. Instrument. The SAR will be an L-band (1.275 GHz), HH polarized system with a 15 MHz bandwidth and a 35 μs pulse width. The antenna size is 11.9 × 2.4 m; this antenna will be folded for launch and deployed in orbit. Data will be acquired at an incidence angle of 38°. The swath width will be 75 km with a resolution of 18 m (3 looks) in the range direction and 18 m in the azimuth direction, and a noise equivalent σ° of −20.5 dB.

2. Data system. Data will be acquired globally on two 30-Mbps recorders and later downlinked to ground receiving stations or downlinked directly at a rate of 60 Mbps. The SAR may be operated on any descending (daytime) node and data may be either downlinked in real time or recorded and downlinked at a later time, depending on ground station coverage. In addition to ERS-1 ground stations, Japan will add two receiving stations in Japan: Hatoyama and Rumamoto. Twenty min of SAR data or 15 min of OPS data may be collected per orbit with a recorder capacity of 20 min.

3. Mission design. The planned sun-synchronous or-

bit has an altitude of 568 km and an inclination of 97.7°, giving a 44-day westward repeat, and thus allowing access to the entire globe with the fixed SAR look angle. The equator crossing time is 10:30–11:00 am and the baseline mission duration is 2 years. The current launch date is February, 1992.

D. RADARSAT

RADARSAT will be Canada's first remote sensing satellite; it will be constructed and launched under the aegis of the Canadian Space Agency in cooperation with the U.S., the provincial governments, and the private sector. The primary objectives of the Canadian RADARSAT mission are to provide application benefits related to offshore oil and gas exploration, ocean fishing, shipping, agriculture, geology, forestry, and land use [56]. RADARSAT will be launched by a NASA-supplied Delta launch vehicle from Vandenburg Air Force Base in 1994.

1. Instrument. The frequency (C-band, 5.3 GHz) and polarization (HH) for RADARSAT have been selected to optimize classification of sea ice. A set of seven beams provides a wide range of incidence angles and swath widths. Resolution is also selectable, depending on the application, with three bandwidths of 11.6, 17.3, or 30.0 MHz available. Fig. 10 shows the coverage of North America with the scanSAR swath in 1 day. Nominal imaging modes include Standard, Fine Resolution, Extended, and ScanSAR (Table V). The C-band system on RADARSAT is a phased array with electronic beam steering in elevation. This is similar to the EOS SAR which will have a fully phased array. Data may be acquired a maximum of 28 min per orbit.

2. Data system. Primary data recovery is through direct downlink at 105 Mbps, although data may be recorded temporarily onboard a tape recorder with a 14-min capacity. Two downlink channels are available, allowing tape-recorded and live data to be handled in parallel through ground receiving stations (Fig. 9). The power budget allows a nominal 28 min of data per orbit period for the SAR. The data collected will be distributed by a private sector company, RADARSAT International (RSI). Data will be collected in Canada at two receiving stations in Prince Albert, Saskatchewan and Gatineau, Quebec.

3. Mission design. RADARSAT is scheduled for launch in 1994 and has a goal of a 5-year mission life. The orbit selected is a dawn/dusk (6 p.m. equator crossing) circular, sun synchronous orbit, thus optimizing the available power through the solar panels and allowing both day and nighttime operation. The nominal altitude is 793–821 km and the inclination is 98.6° resulting in a 24-day repeat cycle with a 7- and 17-day approximate repeats. This orbit allows imaging of any part of the globe between 71.5° and 75.5°N at least once every 24 h and between 51.5° and 71.5° N every 72 h. It also allows imaging agricultural areas at least every 7 days and of the entire global land mass in stereo. Nominally the SAR will be right-looking providing coverage of the Arctic; however, two 2-week periods (winter and summer) with the radar left-looking are planned to map Antarctica during maximum and minimum ice cover. Fig. 10 shows the coverage of North America with the scan SAR swath in 1 day.

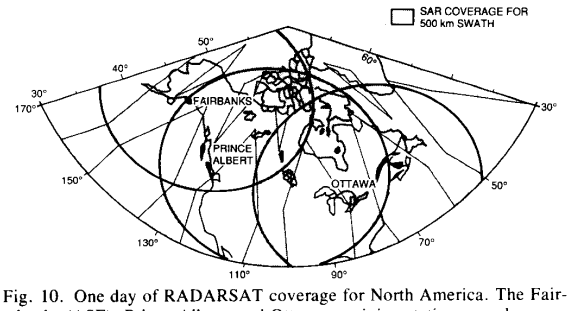

Fig. 10. One day of RADARSAT coverage for North America. The Fairbanks (ASF), Prince Albert, and Ottawa receiving stations are shown.

TABLE V
RADARSAT IMAGING MODES

	Resolution (m × m)*	Looks	Swath (km)	Incidence Angle Range
Standard	28 × 25	4	100	20-40°
Wide (1)	28 × 48-30	4	165	20-31°
Wide (2)	28 × 32-25	4	150	31-39°
Fine Resolution	9 × 11-9	1	45	37-48°
ScanSAR (N)	50 × 50	8	305	20-40°
ScanSAR (W)	100 × 100	4-8	510	20-40°
Extended (H)	28 × 22-19	4	75	50-60°
Extended (L)	28 × 68-28	4	170	100-23°

*azimuth X range

E. Alaska SAR Facility

To support the international spaceborne missions, NASA has developed the Alaska SAR Facility (ASF). This facility is being designed and implemented by JPL and located at and operated by the University of Alaska's Geophysical Institute in Fairbanks, which will receive, process, and distribute the data. The ground system consists of three major subsystems (Fig. 11): the Receiving Ground Station (RGS) (including a large dish antenna located on top of the Geophysical Institute), the SAR Processor System (SPS), and the Archive and Operation System (AOS). In addition, a Geophysical Processor System (GPS) has been added and currently includes three operational algorithms which determine ice motion (Kwok et al., 1990), ice classification (Kwok et al., 1991), and wave properties.

V. PLANETARY RADARS

Synthetic aperture radar data are not only valuable for Earth science studies, but are also important for studying the surfaces of planets and their satellites, particularly of Venus, which is permanently and completely covered with clouds, and Titan, also completely cloud shrouded. Com-

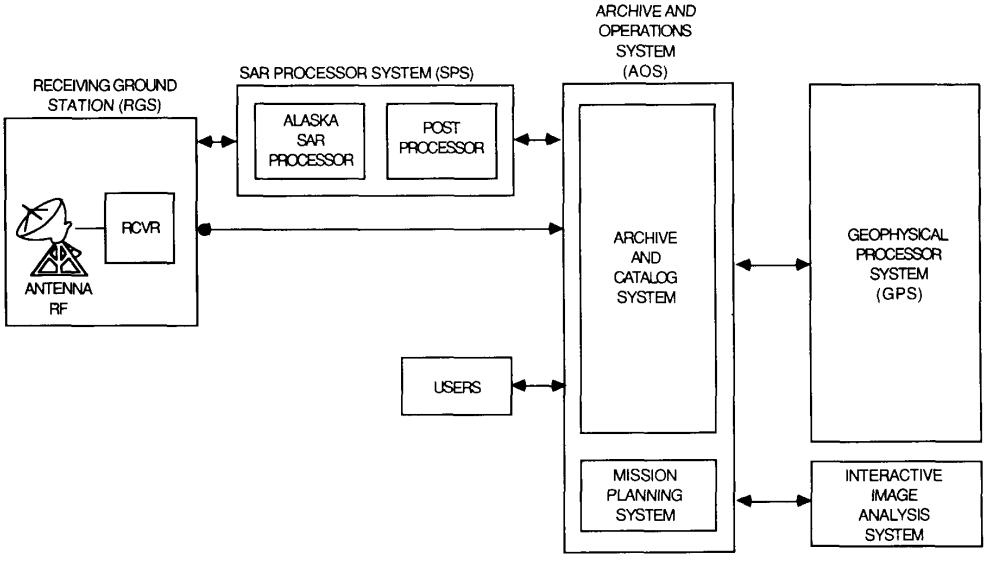

Fig. 11. Functional block diagram for the Alaska SAR Facility (ASF).

parison with SAR data obtained on Earth will provide analogies for the planetary missions. NASA is currently undertaking two planetary radar missions: Magellan to Venus and Cassini to Titan (Table VI).

A. Magellan

Venus was first visited in 1962 by Mariner 2. The first soft landing on Venus was by Venera 7 in 1970 followed by Venera 8 (1972), Venera 9 (1975), and Venera 10 (1975). Pioneer 12 in 1978 carried the first radar to Venus providing the first detailed map of the planet's surface. In 1983, Venera 15 and 16 also provided radar mapping of Venus at 2–4 km resolution.

Magellan was launched on May 4, 1989 from the space shuttle Atlantis (Fig. 12(a)) [60], [61]. The spacecraft maneuvered into Venus orbit on August 10, 1990; the mapping mission began on September 15, 1990. The planet will have been mapped once by May 15, 1991. The primary objectives of the Magellan Venus radar mapping mission are to study (1) the geologic and tectonic history, specifically the surface morphology and surface processes, (2) the geophysics of Venus, principally its density distribution and interior dynamics, and (3) the small-scale surface physics. To meet these objectives, the radar system is designed to produce contiguous images of at least 70% of the planetary surface with a resolution of 500 m or better, surface microwave brightness temperatures to better than 2°, and a topographic map with a height resolution of better than 50 m.

1. Instrument. Magellan is a 3453 kg, three-axis, stabilized spacecraft with an Inertial Upper Stage (IUS). The Magellan radar is an S-band system capable of acquiring burst-mode SAR, altimetry, and passive microwave or radiometer data. The altimetry spatial resolution varies between 20 and 55 km with a height resolution of 30 m. The spatial resolution of the radiometer is greater than 20 km with a temperature resolution of 2K. Together these data will be used to determine surface morphology and electrical properties, which will then be useful in determining the geologic history of Venus by providing a better understanding of tectonic, volcanic, cratering, and erosional processes controlling the formation of the surface.

The SAR system is a hybrid radar utilizing the communication antenna, a Voyager antenna of 3.7 m diameter parabolic reflector. The antenna has 2 feeds: a 13 cm (S-band) feed for the SAR and a 3 cm (X-band) feed for the communications link. The radar also includes an electronic box containing a stable local oscillator (STALO), clock, transmitter, receiver, baseband processor, data formatter, and telemetry and command. Each unit is duplicated and a switch is made by ground command. The total mass is 150 kg with 210 W power from batteries recharged by solar arrays. The bandwidth of the Magellan radar is 2.26 MHz, resulting in a range resolution of 120 m at the low altitudes. The azimuth resolution is held at 120 m at all altitudes. Incidence angles vary through each pass; however, the incidence angle is greater than 30° at all times to avoid layover and foreshortening in mountainous terrain.

2. Data system. The three data types are acquired concurrently by interleaving the data. Data are acquired and recorded at a rate of 806 Kbps (790 Kbps for the radar) as the spacecraft passes behind Venus (relative to the Earth) for a total time of 33 min/orbit and then transmitted to Earth through the same antenna as the orbiter comes into radio contact, with a data rate of 270 Kbps and duration of 112 min. The data volume per orbit is 1700

TABLE VI
THE PLANETARY MISSIONS

	Magellan	Cassini
Imaging Characteristics		
Band (wavelength) cm	S(12.6)	Ku (2.2)
Frequency (GHz)	2.385	13.8
Polarization	HH	HH
Look (Incidence) Angles (deg)	13–46° (18°–50°)	10.5–12.9 (14.0–35.4)
Azimuth Resolution (m)	120–150	600–2100
Range Resolution (m)	120–360	400–1600
Looks	≥4	4–32
Swath (km)	20 (variable)	68–311
Swath Length (km)	16,000 km	TBD
Right/Left Looking	either (left for nominal mission)	both
Instrument Characteristics		
Antenna Type	dish	reflector w/offset feeds
Antenna Size (m diameter)	3.7	3.7
Peak Power (W)	350	65
Bandwidth (MHz)	2.26	0.06–1.0
Orbit Characteristics		
Altitude for Radar Ops (km)	275–2100	1000–4000
Inclination	85.3°	variable
Exact Repeat Cycle	243 days	~32 days (Saturn orbit)
Mission		
Planet/Moon	Venus	Saturn/Titan
Spacecraft	Magellan	Cassini (Mariner Mark II)
Launch Vehicle	Shuttle/IUS	Titan 4/Centaur
Launch Date	May 4, 1989	1996
Orbit Insertion	August 10, 1990	2002
Mission Duration	243 days (nominal)	32 fly-bys in 4 years
Nominal Mission End	May 15, 1991	2006
Data Characteristics		
Record Data Rate (Kbps)	790	365
Recorder Capacity (Mbits)	1700	TBD
Record Time Per Orbit (min)	33	4
Playback Time Per Orbit (min)	112	
Coverage	70% of planet (90% in extended mission)	35–50% of surface
Processing		
Type	digital	digital
Location	JPL	JPL
Processor	Magellan High Rate Processor	
Other Sensors		
	Altimeter Radiometer	Imaging System UV, NIR and Mid-IR Spectrometers High Speed Photometer Dust Analyzer Plasma Detector and Spectrometer Aeronomy Platform

*not including the antenna dish.
**for topographic/stereo mode @ 10-km spatial resolution.

Mbits. Processing of the Magellan data is being done on the JPL Magellan High Rate Processor which is capable of processing large data volumes in near real time.

A total of 3000 Gb of data were collected over the nominal mission. These radar data are being processed into uncontrolled mosaics of images, topography, and refined products including emissivity and RMS slope. The image data are processed into 25 × 16,000 km strips [62]. Mosaics of approximately 15% of the Venus surface with 75 m resolution are then being generated. The entire data set is being converted into three products: 1) 15 × 15° images with 225-m pixels; 2) 45° × 45° images with 675 m pixels; and 3) 80° × 120° images with 2025 m pixels. The Magellan mission will generate more digital data than all previous US planetary missions combined (3×10^{12} bits during the first 243 days).

3. Mission design. The nominal mission lasted one full Venus rotation (243 days) and provided coverage of 70% of the planet's surface. An extended mission is currently in progress which includes additional coverage and an option to obtain multiple incidence angle (stereo) image sets, providing 30 m height resolution topography. The orbit is

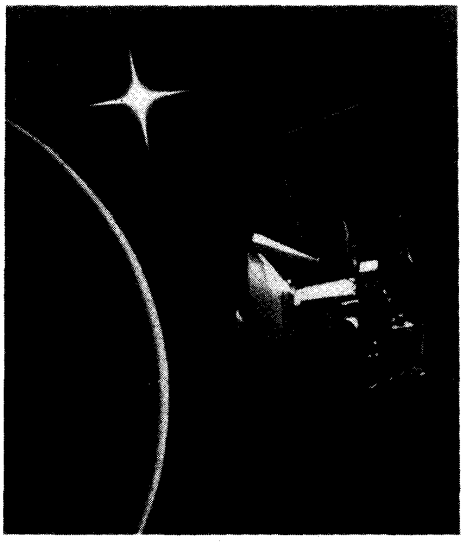

(a)

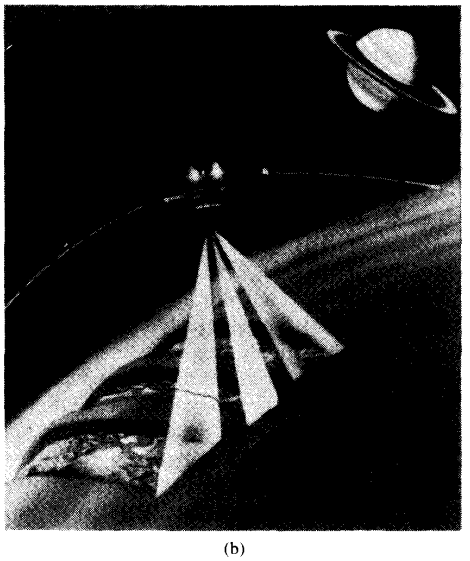

(b)

Fig. 12. The planetary SAR missions including (a) Magellan and (b) Cassini RADAR.

highly elliptical with a 275–2100 km altitude, thus swath and resolution vary with position in the orbit. The orbit is inclined to 85.3° allowing access to 90°N to 67°S. Typically, the 3.15 h orbit (Fig. 13) has a 275-km periapsis altitude at 10°N latitude, resulting in an altitude of 2150 km at the north pole and an 8029 km near 74°S. The radar images between ±80° latitude of the periapsis point (275–2100 km altitude range). In the first Venusian year, the radar was oriented in a left-looking mode providing coverage of the North Pole. The extended mission provides right-looking coverage of the South Pole. The 189-min orbit provides 37 min of radar data acquisition, 112 min of playback, and 40 min for star sighting for attitude reference calibration. The system makes 3,000 changes in its operating mode during each mapping period.

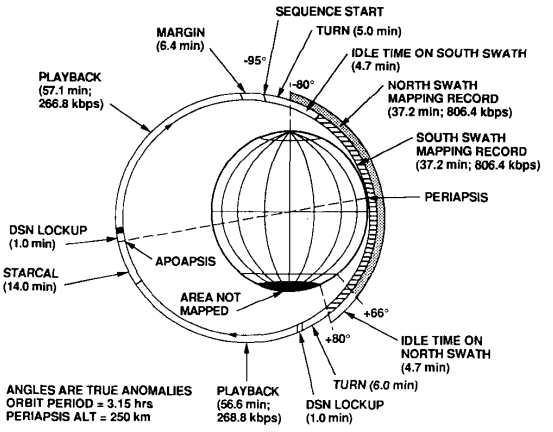

Fig. 13. The orbit for Magellan showing the imaging periods on the far side of Venus and the tape playback periods on the near side.

B. Cassini

The only known planetary satellite with a solid surface which is completely covered with clouds is Titan[2], the largest Saturnian satellite and the second largest moon in the solar system. Potential clouds of methane [63] in the troposphere and a haze of acetylene and polyacetylenes in the stratosphere eliminate any possibility of optically imaging the surface. Irreversible photolytic destruction of methane in the stratosphere [64] may produce ethane, propane, nitrite, and acetylene precipitation [65], [66]. The condensed photolysis products could have formed a liquid or solid surface layer several meters to kilometers thick as Titan evolved [65]–[69]. In 1989, the first radar observations of Titan [70] using the Goldstone X-band radar as the transmitter and the Very Large Array (VLA) in New Mexico as the receiver were made. The observed variability in the measured cross section imply a spatially nonuniform surface.

NASA will launch an Orbiter carrying a radar to Saturn in 1996 on a Titan IV with a Centaur upper stage (Fig. 12(b)). The goal of the Titan portion of the mission is to determine the physical state, topography and composition of the surface and infer the internal structure. The orbiter will carry a Titan Huygens Probe provided by ESA; the two make up the Cassini mission, the second of the Mariner Mark II series of outer planet and primitive bodies missions. The Cassini mission will be combined with the Comet Rendezvous/Asteroid Flyby (CRAF) mission to make up the CRAF/Cassini mission.

1. Instrument. The Cassini RADAR is as a facility instrument for the Cassini mission [71], [72]. In the current baseline RADAR consists of two operational modes, including an imaging SAR mode for surface imaging at high resolution, and a nadir-viewing altimeter (ALT) mode for

[2]Titan's radius is 2,578 km, its surface temperature is ~94K, and its surface pressure is ~1.5 bars.

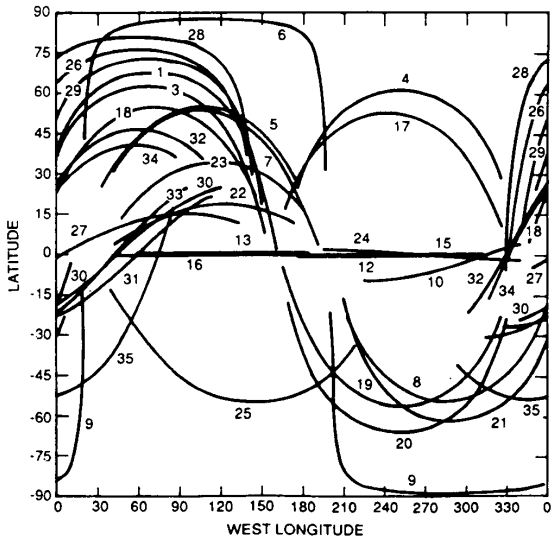

Fig. 14. Ground tracks of the Titan flybys for altitudes below 8000 km during a representative Saturn System Tour.

obtaining topographic information at 30 m vertical resolution.

The radar will operate at Ku-band (13.8 GHz) utilizing the 3.66-m diameter, high-gain telecommunications antenna reflector. Imaging will be possible on either side of nadir. The high resolution SAR mode will be operated at closest approach. Medium-resolution imaging will be done during the inbound and outbound legs. Scatterometry and altimetry data will be collected for the duration of the flyby.

2. Data system. RADAR measurements will be collected in approximately 32 close flybys over Titan. The raw radar data will be recorded on the Orbiter's tape recorder at the maximum rate of 365 Kbps, and later transmitted to Earth for processing and analysis. A total of about 16 Gb of raw data will be collected over the nominal mission. In the preliminary plan, these radar data will be processed into mosaics of images, topography, and surface backscatter cross-sections.

3. Mission design. The Saturn Orbiter will release a probe to Titan once it reaches Saturn and will then make repeated passes over Titan during its 4-year nominal mission. During this 4-year lifetime, the Saturn orbiter will orbit Saturn 59 times with a period of approximately 32 days; the configuration of each orbit will be determined by approximately 35 Titan gravity-assist flybys. Of the 35 flybys, approximately 32 will reach altitudes below 8000 km (i.e., altitudes useful for radar imaging) at some point during the pass, with the lowest altitude of 950 km. The first must be at about 1500 km to reduce the spacecraft orbital period and inclination. The RADAR will operate for approximately 60 min, centered around closest approach, covering approximately 30% of Titan's surface. Fig. 14 shows one scenario for flyby groundtrack coverage.

VI. EOS SAR

A. Evolution of Synthetic Aperture Radar to the EOS SAR Design

The evolution of the spaceborne imaging radars has lead to a multipolarization, multifrequency system with variable imaging geometry which will be ready for flight as part of the Earth Observing System (EOS) mission at the end of the 1990s (Fig. 15). Nominally, this SAR will be a three-frequency (L-, C-, and X-bands) system with quadpolarization available for the L-band and dual polarization for C- and X-bands. The SAR will be capable of acquiring multiincidence angle and scanSAR data using electronic beam steering. The EOS SAR will provide a unique new data set as well as continuity with the international missions, and will play a key role in understanding the Earth's global processes alone and synergistically with the complement of EOS instruments.

B. Description

The EOS SAR is part of the multiplatform EOS mission to study global change (Fig. 16). The U.S. contribution to the spaceborne portion of the EOS mission includes two multiinstrument polar platforms—EOS-A and EOS-B—and a dedicated EOS SAR platform. The EOS-A and EOS-B platforms are part of a 1991 new start. The new start for the EOS SAR will follow such that the SAR and EOS-A fly concurrently.

1. Instrument. The current design for the EOS SAR includes an L-band quad polarization and C- and X-band dual polarization (HH, VV, and phase) systems. The X-band SAR, X-EOS [73], [74] will be provided by Germany. Although it is desirable to fly a permanently orbiting SAR with the full frequency, full polarization capability from the higher altitudes required for a long duration mission (600–800 km), mass limitations on the launch vehicle (a Delta-class launcher) constrain the EOS SAR design. The antenna for the EOS SAR as currently planned is 2.6 m in width and 10.9 m in length. All three antennas are distributed; the antennas will be fixed on the right-hand side looking in the northward direction to optimize polar sea ice imaging. Multiple incidence angle data may be acquired by electronic steering. It will also be possible to mechanically roll the antenna to look south for selected periods of time. The radar will have a peak power of 5.8 kW to be distributed between the three systems in a variety of modes as described in Table II. With these power limitations, the maximum incidence angle in the single polarization mode (transmit either H or V) is 45° and in the dual and quad polarization modes (transmit H and V) is 30°.

It is desirable to obtain global coverage as frequently as possible with the EOS SAR. With the above incidence angle range, a 360-km swath is possible (single polarization) in the scanSAR mode resulting in near global coverage every 5 days (Fig. 17). Although nearly any combination of swath and resolution is feasible within the peak data rate constraints, three nominal modes have been se-

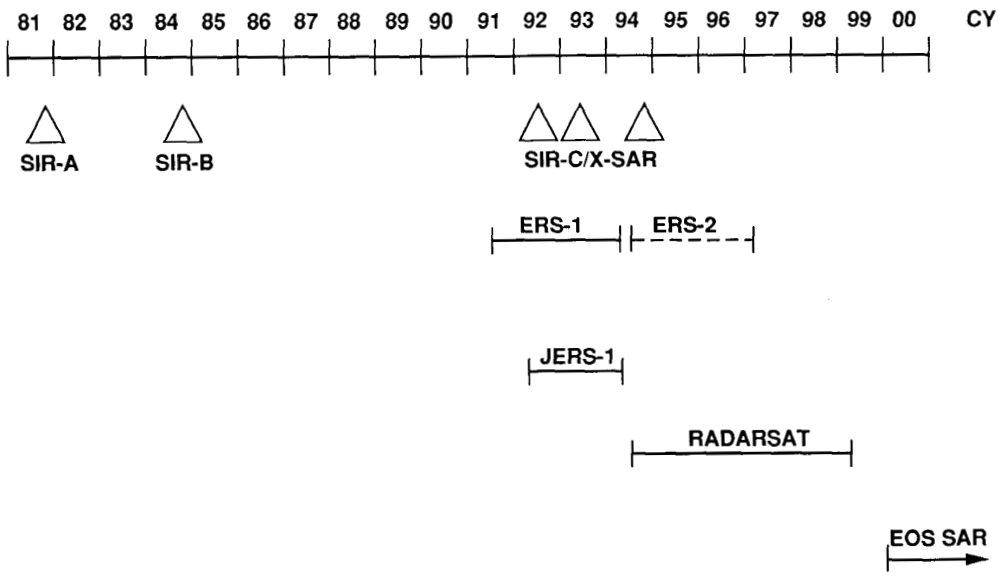

Fig. 15. The schedule for the spaceborne SAR missions from Seasat through the EOS SAR.

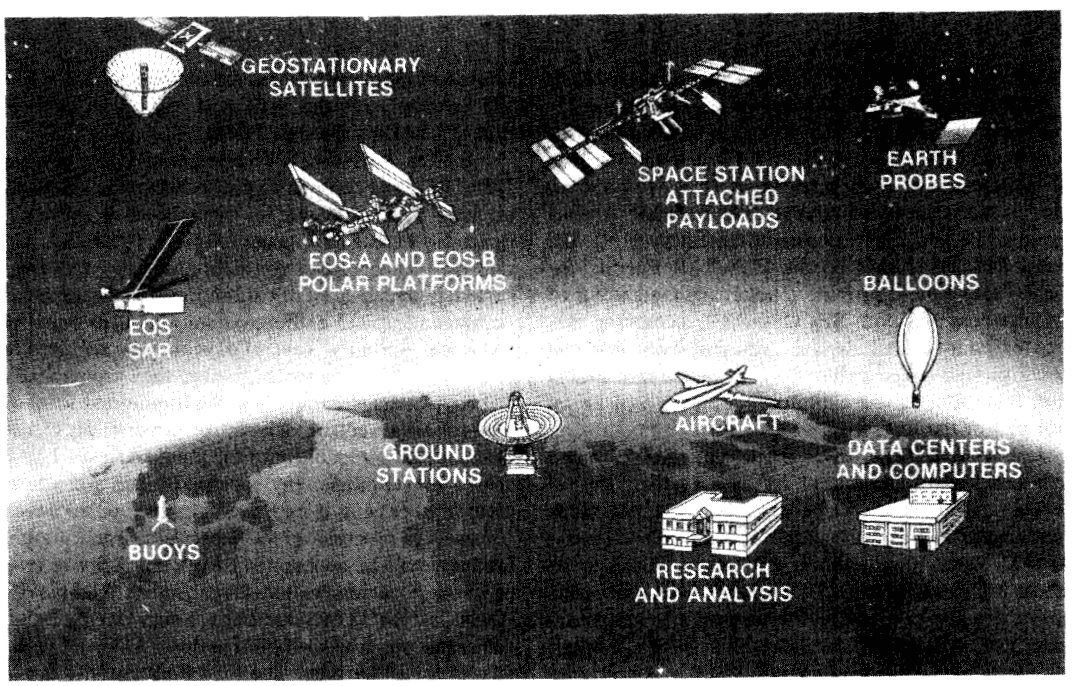

Fig. 16. Diagram of the EOS mission including the EOS-A and EOS-B platforms, the EOS SAR, the Earth probes, the Space Station, and the Geostationary Satellites. Also shown are the ground segments and aircraft and balloon experiments.

lected: Local High Resolution (20–30 m resolution, 30–50 km swath), Regional Mapping (50–100 m, 100–200 km) and Global Mapping (250 m, 360 km). In order to optimize swath width and reduce data rates, it will be possible to select between a range of bandwidths.

As with SIR-C/X-SAR, calibration over the lifetime of

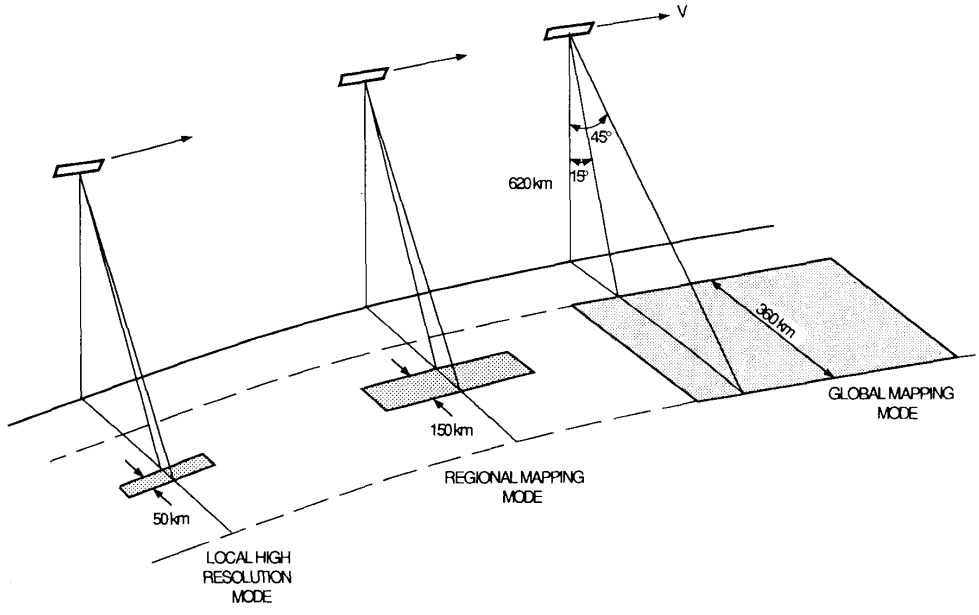

Fig. 17. The three imaging modes for the EOS SAR including the Local High Resolution, the Regional Mapping, and the Global Mapping modes.

EOS is essential, particularly since a primary goal for EOS is to compare data sets collected over the full nominal 15-year lifetime. In addition, it is desirable to obtain a relative calibration between the EOS SAR and the international SAR missions, which began in 1991, in order to monitor phenomena which change over decades. An initial estimate of this calibration requirement is +/−1 dB; however, detailed studies by the EOS SAR Facility Instrument Team should provide a better understanding of this requirement. As with SIR-C/X-SAR, achieving this level of calibration will require preflight, onboard, and extensive ground-based calibration. A permanent global network of ground-based calibration stations will be an integral part of the EOS SAR system.

2. Data system. The EOS SAR will take a much needed step toward improving its data system; the 50 Mbps Ku-band antenna will be replaced by a 300 Mbps Ku-band antenna. Inasmuch as the TDRS satellite is limited to 300 Mbps, this addition will allow TDRS to be used to its full capacity (Fig. 2). The EOS SAR spacecraft will also carry a very high data rate recorder to temporarily store data which will be later downlinked through TDRS. Once the data arrive at White Sands, they must be buffered to 50 Mbps to be sent through Domsat to JPL for processing.

In the present EOS SAR design, each single polarization, single frequency, 4 look, 6 bps channel requires about 100 Mbps to acquire a 100 km swath. The combined Local High Resolution and Regional Mapping modes require a yearly average data rate of about 10 Mbps based on a representative data acquisition plan. The Global Mapping Mode requires an additional 5 Mbps on the average, thus the SAR will require an average data rate of 15 Mbps through TDRS.

All EOS SAR data will be operationally processed to Level 1 [75] or calibrated, geocoded images implying that all EOS SAR data will be operationally calibrated and geocoded before any image output is produced. The current plan for operationally calibrating the data is to continuously update a set of calibration tables generated using permanent ground calibration stations distributed around the world. Initially, several days may be required to generate the calibration tables, before they are applied to the EOS SAR data stream. Thus, the turnaround for the Level 1 processing may be delayed by several days, although the processing capability of the planned Level 1 SAR processor will eliminate any backlog of data and allow complete reprocessing if improved algorithms are developed.

Level 2 processing to geophysical and biophysical products will be accomplished operationally at two SAR processing centers called Data Active Archive Centers (DAACs): EROS in Sioux Falls, South Dakota for all land data, and the Alaska SAR Facility (ASF) in Fairbanks, Alaska for all ice data. The EOS SAR Facility Instrument Team is responsible for developing the algorithms for the operational geophysical processors. The Level 2 output will be sent to the EOS Data and Information System (EOSDIS) for distribution to EOS and other investigators for use in regional and global models.

3. Mission design. Possible orbit altitudes for the EOS-A and EOS-B have changed several times over the past few years [76], but both are sun-synchronous and

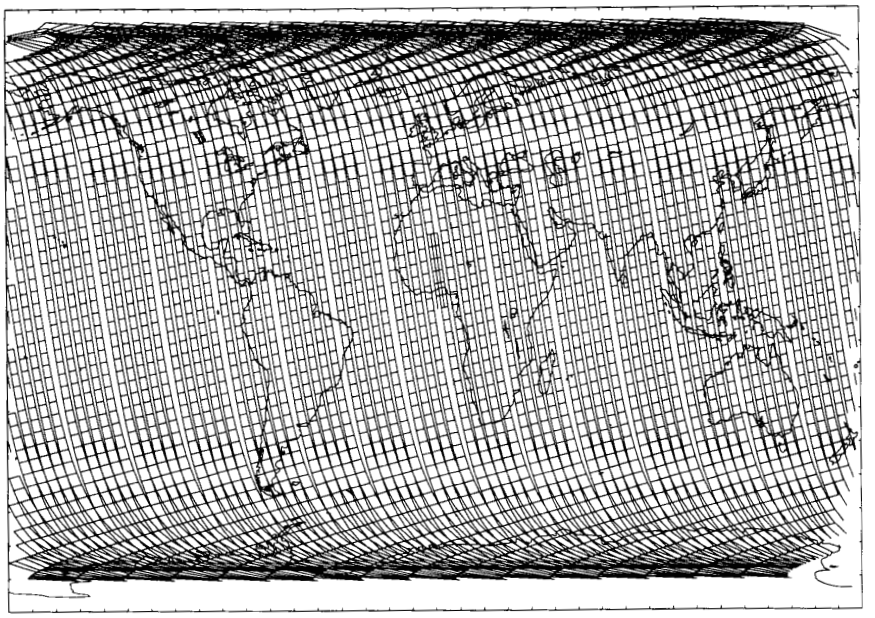

Fig. 18. The 620 km orbit option for the EOS SAR; a 360-km Global Mapping Mode swath is used; the SAR is right looking and 5 days of coverage are plotted. Tick marks are for 1 min.

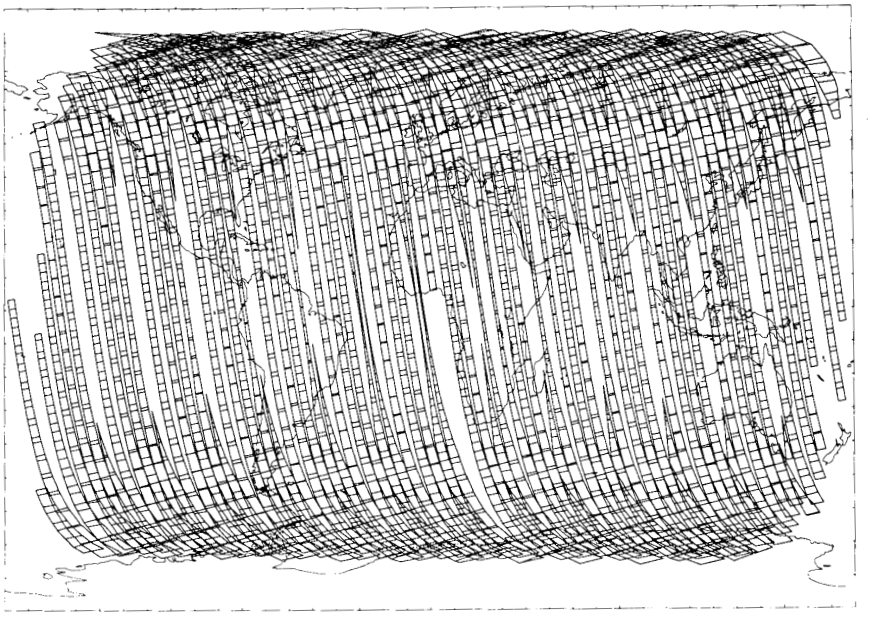

Fig. 19. Simultaneous coverage by the EOS SAR (Global Mapping Mode) at 620 km and MODIS-N at 700 km assuming a 60-min simultaneity requirement. Days 1–5 are plotted with 1-min tick marks.

therefore approximately 98° inclination. The current baseline is a 700 km orbit; a skipping 16-day repeat cycle orbit which provides coverage similar to a 2-day repeat cycle orbit. This orbit is preferred for wide field of view EOS instruments which desire global coverage every 2 days. With the EOS SAR on its own spacecraft, it is possible to select any altitude. It is desirable to fly at the same altitude and inclination as EOS-A (where the nadir-look-

ing optical instruments including the High Resolution Imaging Spectrometer, HIRIS, and the Moderate Resolution Imaging Spectrometer, MODIS, are located) with some equator crossing offset to optimize synergism between the SAR and nadir-looking instruments. However, mass constraints imply a lower altitude is preferred to reduce the size of the SAR antenna. The current baseline is 620 km (Fig. 3); a 16-day exact repeat orbit with an approximate 5-day repeat (Fig. 18). With the different SAR and EOS platform altitudes, consistent synergism is lost, although over a 5-day period much of the Earth is accessible within 60 min by both platforms (Fig. 19).

VI. Summary

The Spaceborne Imaging Radar program has evolved through Seasat and the Shuttle Imaging Radar (SIR) to a multifrequency, multipolarization system capable of monitoring the Earth with a variety of imaging geometries, resolutions, and swaths. In particular, the ability to digitally process and calibrate the data has been a key factor in developing the algorithms which will operationally provide geophysical and biophysical information about the surface of the Earth using synthetic aperture radar (SAR). This paper has discussed the missions leading up to the EOS SAR as well as the international spaceborne and aircraft missions which are an integral part of the imaging radar program.

Acknowledgment

The authors would like to thank Ben Holt, Charles Elachi, Wu Yang Tsai, Rolando Jordan, Walt Brown, Ed Caro, Steve Wall, Eastwood Im, John Curlander, Daren Casey, Annie Richardson, Laci Roth, and Marguerite Schier of the Jet Propulsion Laboratory, Keith Carver of the University of Massachusetts, Eric Kasischke of the Environmental Institute of Michigan, Herwig Ottl of DLR in Germany, and Keith Raney, Laurence Glay, and Ron Brown of the Canada Centre for Remote Sensing for their valuable comments. This work was carried out at the Jet Propulsion Laboratory, California Institute of Technology, for the National Aeronautics and Space Agency.

References

[1] M. Schier and J. B. Way, "*The earth observing system interdisciplinary science objectives and data products*," Jet Propulsion Laboratory, California Institute of Technology, JPL Pub. D-7931, 1990.

[2] D. E. Weissman Ed., Seasat-1, Special Issue of the *IEEE J. Oceanic Eng.*, vol. OE-5, 1980.

[3] R. L. Jordan, "The Seasat-A synthetic aperture radar system," *IEEE J. Oceanic Eng.*, vol. OE-5, no. 2, p. 154, 1980.

[4] E. Pounder, "*Seasat final report, vol. I-IV*," Jet Propulsion Laboratory, California Institute of Technology, JPL Pub. 80-38, 1980.

[5] G. H. Born, J. A. Dunne, and D. B. Lame, "Seasat mission overview," *Science*, vol. 204, pp. 1405–1406, 1979.

[6] F. I. Gonzalez, *et al.*, "Seasat synthetic aperture radar: Ocean wave detection capabilities," *Science*, vol. 204, pp. 1418–1424, 1979.

[7] J. P. Ford, R. G. Blom, M. G. Bryan, M. I. Daily, T. H. Dixon, C. Elachi, and E. C. Xenos, "*Seasat views North America, the Caribean, and Western Europe with Imaging Radar*," Jet Propulsion Laboratory, California Institute of Technology, JPL Pub. 80-67, 1980.

[8] L. Fu, and B. Holt, "*Seasat views oceans and sea ice with synthetic aperture radar*," Jet Propulsion Laboratory, California Institute of Technology, JPL Pub. 81-120, 1982.

[9] T. D. Allan, Ed., *Satellite Microwave Remote Sensing*. New York: John Wiley.

[10] A. D. Kirwan, T. J. Ahrens, and G. H. Bern, Eds., Seasat Special Issue II of the *J. Geophys. Res.*, vol. 88(C3), 1983.

[11] F. Carsey and B. Holt, "Beaufort-Chukchi ice margin data from Seasat: Ice motion," *J. Geoph. Res.*, vol. 92, pp. 7163–7172, 1987.

[12] R. Beal, Ed., "*Measuring ocean waves from space*," Johns Hopkins APL Tech. Dig., vol. 8, no. 1, 1987.

[13] R. Beal, P. S. DeLeonibus, and I. Katz, Eds., "*Spaceborne synthetic aperture radar for oceanography*," Tech. Dig., Johns Hopkins APL, Baltimore, 1981.

[14] R. L. Bernstein, Ed., Seasat Special Issue I of the *J. Geophys. Res.*, 87(C5), 1982.

[15] J. Businger and R. H. Stewart, Eds., *Seasat-JASIN Workshop Report*, Vol. I, Jet Propulsion Laboratory, California Institute of Technology, JPL Pub. 80-62, 1980.

[16] C. Wu, B. Barkan, B. Huneycutt, C. Leang, and S. Pang, "*An introduction to the interim digital SAR processor and the characteristics associated with SEASAT SAR images*," Jet Propulsion Laboratory, California Institute of Technology, JPL Pub. 81-26, 1981.

[17] S. H. Pravdo, B. Huneycutt, B. Holt, and D. H. Held, "*Seasat synthetic aperture radar data users manual*," Jet Propulsion Laboratory, California Institute of Technology, JPL Pub. 82-90, 1982.

[18] J. C. Curlander, R. Kwok, and S. S. Pang, "A post-processing system for rectification and registration of spaceborne SAR imagery," *Int. J. Rem. Sens.*, vol. 8, 621–638, 1987.

[19] J. B. Cimino and C. Elachi, Ed., *The Shuttle Imaging Radar-A (SIR-A) Experiment*, Jet Propulsion Laboratory, California Institute of Technology, JPL Pub. 82-77, 1982.

[20] C. Elachi, W. E. Brown, J. B. Cimino, T. Dixon, D. L. Evans, J. P. Ford, R. S. Saunders, C. Breed, H. Masursky, J. F. McCauley, G. Schaber, L. Dellwig, A. England, H. MacDonald, P. Martin-Kaye, and F. Sabins, "Shuttle Imaging Radar experiment," Science, vol. 218, pp. 996–1003, 1982.

[21] M. Settle and J. Taranik, "Use of the space shuttle for remote sensing research: Recent results and future prospects," *Science*, vol. 218, pp. 993–995, 1982.

[22] J. Ford, J. B. Cimino, and C. Elachi, "*Space shuttle Columbia views the world with imaging radar: The SIR-A experiment*," Jet Propulsion Laboratory, California Institute of Technology, JPL Pub. 82-95, 1982.

[23] J. F. McCauley, G. G. Schaber, C. S. Breed, M. J. Grolier, C. U. Haynes, B. Issawi, C. Elachi, and R. Blom, "Subsurface valleys and geoarchaeology of the eastern Sahara revealed by Shuttle Radar," *Science*, vol. 218, pp. 1004–1019, 1982.

[24] J. F. McCauley, C. S. Breed, G. G. Schaber, W. P. McHugh, B. Issawi, C. V. Haynes, M. J. Grolier, and A. El Kilani, "Paleodrainages of the eastern Sahara—The radar rivers revisited (SIR-A/B implications for a mid-tertiary trans-African drainage system)," *IEEE Trans. Geosci. Rem. Sens.*, GE-24, pp. 624–648, 1986.

[25] G. G. Schaber, J. F. McCauley, C. S. Breed, and G. R. Olhoeft, "Shuttle Imaging Radar: Physical controls on signal penetration and subsurface scattering in the eastern Sahara," *IEEE Trans. Geosci. Rem. Sens.*, GE-24, pp. 603–623, 1986.

[26] SIR-B Science Team, Ed., "*The SIR-B science investigations plan*," Jet Propulsion Laboratory, California Institute of Technology, JPL Pub. 84-3, 1984.

[27] J. B. Cimino, C. Elachi, and M. Settle, "SIR-B—The second shuttle imaging radar experiment," *IEEE Trans. Geosci. Rem. Sens.*, GE-24, pp. 445–452, 1986.

[28] J. P. Ford, J. B. Cimino, B. Holt, and M. Ruzek, "*Shuttle imaging radar views the earth from Challenger: The SIR-B experiment*," Jet Propulsion Laboratory, California Institute of Technology, JPL Pub. 86-10, 1986.

[29] J. B. Cimino, B. Holt, and A. Richardson, *The SIR-B experiment report*, Jet Propulsion Laboratory, California Institute of Technology, JPL Pub. 87-88-2, 1987.

[30] C. Elachi, Ed., SIR-B Special Issue of the *IEEE Trans. Geosci. Rem. Sens.*, GE-24, 1986.

[31] M. C. Dobson, F. T. Ulaby, D. R. Brunfeldt, and D. N. Held, "External calibration of SIR-B imagery with area-extended and point targets," *IEEE Trans. Geosci. Rem. Sens.*, GE-24, pp. 453–461, 1986.

[32] C. Elachi, J. B. Cimino, and M. Settle, "Overview of the Shuttle

Imaging Radar-B preliminary scientific results," *Science*, vol. 232, 1986.
[33] B. Holt, Ed., Special Issue on Shuttle Imaging Radar experiment, *J. Geophys. Res.*, vol. 33, 1988.
[34] J. P. Ford, Ed., Special Issue on Advances in Shuttle Imaging Radar-B Research, *Int. J. Rem. Sens.*, vol. 9, 1988.
[35] "Shuttle Imaging Radar-C Science Plan," JPL Pub. 86-29, 1986.
[36] R. L. Jordan, B. L. Huneycutt, and M. Werner, "The SIR-C/X-SAR Synthetic Aperture Radar System," *Proc. IEEE*, vol. 79, no. 6, pp. 827–838.
[37] D. Evans and C. Elachi, "Overview of the Shuttle Imaging Radar (SIR-C)," *IGARSS'88*, Edinburgh, Scotland.
[37a] H. Öhl and Valdoni, *The X-SAR Science Plan*, 1985.
[38] M. Wahl and P. Ammendola, "Main features of the X-SAR project," *IGARSS'88*, Edinburgh, Scotland.
[39] E. H. Velten, "A new spaceborne Synthetic Aperture Radar," in *Proc. IGARSS'88*, Edinburgh, Scotland.
[40] H. Ottl, "Scientific Goals and Technical Limitations of the Shuttleborne Synthetic Aperture Experiment X-SAR," *Proc. 15th Int. Symp. Space Technology and Science*, Tokyo, Japan, pp. 1699–1704, 1986.
[41] H. Ottl and M. Werner, "Gernam Synthetic Aperture Radar Activities for shuttleborne missions," in *Proc. 14th Int. Symp. Space Technology and Science*, Tokyo, Japan, pp. 1301–1306, 1984.
[42] R. Horn, "C-band SAR results obtained by an experimental airborne SAR sensor," *IGARSS'89*, pp. 2213–2216.
[43] T. W. Thompson, "*NASA/JPL aircraft SAR operations for 1984 and 1985*," Jet Propulsion Laboratory, California Institute of Technology, JPL Pub. 86-20, 1986.
[44] van Zyl, *et al.*, *AIRSAR Reference Manual*. Jet Propulsion Laboratory, California Institute of Technology, JPL Pub. 1991.
[45] A. D. Kozma, A. D. Nichols, R. F. Rawson, S. J. Schackman, C. W. Haney, and J. J. Shanne, Jr., "Multifrequency, multipolarization SAR for remote sensing," *Proc. IGARSS'86*, Zurich, Switzerland, ref. ESA SP-254, pp. 715–719.
[46] R. Sullivan, A. Nichols, R. Rawson, C. Haney, F. Darreff, and J. Schanne, Jr., "Polarimetric X/L/C-Band SAR," in *Proc. 1988 IEEE Radar Conf.*, Ann Arbor, MI, pp. 9–14.
[47] C. E. Livingstone, A. L. Gray, R. K. Hawkins, J. G. Halbertema, R. A. Deane, and R. B. Olson, "CCRS C-Band airborne Radar-Systems Description and Test Results," in *Proc. 11th Canadian Symp. Remote Sensing*, Waterloo, Ontario, p. 36, 1987.
[48] C. E. Livingstone, A. L. Gray, R. K. Hawkins, and R. B. Olsen, "CCRS C-X-Airborne Synthetic Aperture Radar: An R and D Tool for the ERS-1 time frame," *IEEE AES*, pp. 11–16, 1988.
[49] "Buyers Guide, Almaz Radar Remote Sensing Satellite," Space Commerce Corp., Houston, TX, 1990.
[50] P. Goldsmith, ERS-1 Special Issue of ESA Bulletin, no. 65, Feb. 1991.
[51] E. P. W. Attena, "The Active microwave instrument, on-board the ERS-1 satellite," *Proc. IEEE*, vol. 79, no. 6, pp. 791–799.
[52] G. Weller, F. Carsey, B. Holt, D. Rothrock, and W. Weeks, "*Science program for an imaging radar receiving station in Alaska, Report of the Science Working Group*," Jet Propulsion Laboratory, California Institute of Technology, JPL Pub. D400-207, 1983.
[53] F. Carsey, Ed., "*Alaska SAR facility science requirements for the receiving ground station, the SAR processor system, and the archive and operations system*," Jet Propulsion Laboratory, California Institute of Technology, JPL Pub. D-3668, 1988.
[54] Alaska SAR Facility Prelaunch Science Working Team Ed., "*Science plan for the Alaska SAR facility program*," Jet Propulsion Laboratory, California Institute of Technology, JPL Pub. 89-14, 1988.
[55] Y. Nemoto, H. Nishino, M. Ono, H. Mizutamari, K. Nishikawa, and K. Tanaka, "Japanese Earth Resources Satellite-1 Synthetic Aperture Radar," *Proc. IEEE*, vol. 79, no. 6, pp. 800–809.
[56] R. K. Raney, A. P. Luscombe, E. J. Langham, and S. Ahmed, "RADARSAT," *Proc. IEEE*, vol. 79, no. 2, pp. 839–849, 1991.
[57] R. Kwok, J. C. Curlander, R. McConnell, and S. Pang, "An ice motion tracking system at the Alaska SAR facility," *IEEE J. Oceanic Eng.*, vol. 15, pp. 44–54, 1990.
[58] R. Kwok, E. Rignot, B. Holt, and R. Onsott, "Classification of sea ice types in spaceborne SAR data," *J. Geophys. Res.*, in press, 1991.
[59] R. S. Saunders, G. H. Pettengill, R. E. Arvidson, W. L. Sjogren, W. T. K. Johnson, and L. Pieri, "The Magellan Venus Radar Mapping Mission," *J. Geophys. Res.*, vol. 95, pp. 8339–8355, 1990.
[60] C. Young, Ed., "*The Magellan Venus Explorer's Guide*," Jet Propulsion Laboratory, California Institute of Technology, JPL Pub. 90-24, 1990.
[61] "EOS SAR Instrument Panel Report, 1988," NASA Document.
[62] R. S. Saunders and G. H. Pettingill, "Magellan: Mission summary," *Science*, vol. 252, pp. 247–249, 1991.
[63] W. T. K. Johnson, "Magellan Imaging Radar Mission to Venus," *Proc. IEEE*, Vol. 79, no. 6, pp. 777–790, 1991.
[64] O. B. Toon, C. P. McKay, R. Courtin, and T. P. Ackerman, "Methane rain on Titan," *Icarus*, vol. 75, pp. 255–284, 1988.
[65] Y. L. Yung, M. Allen, and J. P. Pinto, "Photochemistry of the atmosphere of Titan: comparison between model and observations," *Astrophys. J.*, vol. 55, pp. 465–506, 1984.
[66] C. Sagan and S. F. Dermott, "The tide in the sea of Titan," *Nature*, vol. 300, pp. 731–733, 1982.
[67] J. Lunine, D. Stevenson, and Y. Yung, "Ethane ocean on Titan," *Science*, vol. 222, pp. 1229–1230, 1983.
[68] V. R. Eschelman, G. G. Lindal, and G. L. Tyler, "Is Titan wet or dry?," *Science*, vol. 221, pp. 53–55, 1983.
[69] F. M. Flaser, "Oceans on Titan?" *Science*, vol. 221, pp. 55–57, 1983.
[70] E. Lellouch, A. Coustenis, D. Gautier, E. Raulin, N. Dubouloz, and C. Frere, "Titan's atmosphere and hypothesized ocean: A reanalysis of the Voyager 1 radio occultation and IRIS 7.7 mm data," *Icarus*, vol. 79, pp. 328–349, 1989.
[71] D. O. Muhleman, A. W. Grossman, B. J. Butler, and M. A. Slade, "Radar reflectivity of Titan," *Science*, vol. 248, pp. 975–980, 1990.
[72] OSSA, "*Cassini Mission: Saturn Orbiter Proposal Information Package, Volume VIII: Titan Radar Mapper Description*," Office of Space Science and Applications, Announcement of Opportunities, Jet Propulsion Laboratory, California Institute of Technology, JPL Pub. D-6464, 1989.
[73] C. Elachi, E. Im, L. E. Roth, and C. L. Werner, "Cassini Titan Radar Mapper," *Proc. IEEE*, submitted.
[74] O. Bender, W. Gilig, and H. Öttl, "X-Band Synthetic Aperture Radar for earth observation satellites (X-EOS)," *IGARSS'90*, pp. 2289–2294.
[75] W. Jatsch, E. Langer, H. Öttl, and K. H. Zeller, "Concept of an X-Band Synthetic Aperture Radar for earth observing satellites," *J. Electromagnetic Waves and Applic.*, vol. 4, no. 4, pp. 325–340, 1990.
[76] J. C. Curlander, "The Earth Observing System (EOS) SAR Ground Data System," Proc. SPIE, p. 1101, 1989.
[77] D. Casey and J. B. Way, "Orbit selection for the EOS mission and its synergism implications," *IEEE Trans. Geosci. and Rem. Sens.*, vol. 29, no. 6, pp. 822–835, Nov. 1991.

JoBea Way, for a photograph and biography please see p. 820 of this TRANSACTIONS.

Elizabeth Atwood Smith received the Bachelor of Science degree in applied and engineering physics from Cornell University, Ithaca, NY, in 1985.

From 1985–1990 she was a member of technical staff at the Jet Propulsion Laboratory, Pasadena, CA, participating in mission and science planning for the Shuttle Imaging Radar (SIR) and Earth Observing System (EOS) projects. She also worked at the Infrared Processing and Analysis Center (IPAC). She now operates a beef cattle farm in Michigan and studies music.